Dynamin and endocytosis are required for the fusion of osteoclasts and myoblasts

Nah-Young Shin,[1,2] Hyewon Choi,[1,2] Lynn Neff,[1,2] Yumei Wu,[3,4] Hiroaki Saito,[1,2] Shawn M. Ferguson,[3,4] Pietro De Camilli,[3,4,5] and Roland Baron[1,2]

[1]Department of Medicine, Harvard Medical School, Boston, MA 02115
[2]Department of Oral Medicine, Infection and Immunity, Harvard School of Dental Medicine, Boston, MA 02115
[3]Department of Cell Biology and [4]Program in Cellular Neuroscience, Neurodegeneration and Repair, Yale School of Medicine, New Haven, CT 06510
[5]Howard Hughes Medical Institute, Chevy Chase, MD 20815

Cell–cell fusion is an evolutionarily conserved process that leads to the formation of multinucleated myofibers, syncytiotrophoblasts and osteoclasts, allowing their respective functions. Although cell–cell fusion requires the presence of fusogenic membrane proteins and actin-dependent cytoskeletal reorganization, the precise machinery allowing cells to fuse is still poorly understood. Using an inducible knockout mouse model to generate dynamin 1– and 2–deficient primary osteoclast precursors and myoblasts, we found that fusion of both cell types requires dynamin. Osteoclast and myoblast cell–cell fusion involves the formation of actin-rich protrusions closely associated with clathrin-mediated endocytosis in the apposed cell. Furthermore, impairing endocytosis independently of dynamin also prevented cell–cell fusion. Since dynamin is involved in both the formation of actin-rich structures and in endocytosis, our results indicate that dynamin function is central to the osteoclast precursors and myoblasts fusion process, and point to an important role of endocytosis in cell–cell fusion.

Introduction

In multicellular organisms, cell–cell fusion is a highly evolutionarily conserved process that leads to the formation of multinucleated cells including myotubes, syncytiotrophoblasts, and osteoclasts. Multinucleation is required for the specific functions of these cells in muscle, placenta, and bone, respectively.

Although it is now well established in *Caenorhabditis elegans* and in the placenta that cell–cell fusion requires the presence of fusogenic membrane proteins (Chen et al., 2007; Oren-Suissa and Podbilewicz, 2007; Helming and Gordon, 2009; Pérez-Vargas et al., 2014), the precise mechanism by which the plasma membranes of two isotypic cells fuse, thus allowing the merging of their cytosolic and nuclear components into a single multinucleated cell, is still poorly understood. Although fusogens for *C. elegans* (Eff-1 and Aff-1; Mohler et al., 2002; Podbilewicz et al., 2006; Sapir et al., 2007; Pérez-Vargas et al., 2014) and for syncytiotrophoblasts (syncytins; Dupressoir et al., 2012) have been identified and characterized, little is known about fusogens in osteoclast precursors (OCPs) and myoblasts cell fusion. For instance, despite the identification of several proteins that are possibly involved in the fusion of OCPs (Mbalaviele et al., 1995; Saginario et al., 1998; Vignery, 2005; Yagi et al., 2005; Lee et al., 2006; Chen et al., 2007; Yang et al., 2008; Gonzalo et al., 2010), their exact role in the cell fusion process has not been characterized.

Besides fusogenic proteins, recent studies have revealed a key role for actin reorganization and podosome-like structures in the fusion of both myoblasts and OCPs (Sens et al., 2010; Abmayr and Pavlath, 2012; Oikawa et al., 2012). Podosomes are highly dynamic structures enriched in F-actin, integrins, and actin-regulating proteins that are involved in many cellular processes, including cell adhesion, motility, and invasion (Linder and Aepfelbacher, 2003; Jurdic et al., 2006; Murphy and Courtneidge, 2011). Actin-regulatory/scaffolding molecules including DOCK180, Rac1, N-WASP, and TKS5/Fish (Pajcini et al., 2008; Gonzalo et al., 2010; Gruenbaum-Cohen et al., 2012;

Correspondence to Roland Baron: Roland_Baron@hms.harvard.edu

Abbreviations used in this paper: 4OHT, 4-hydroxytamoxifen; BMM, bone marrow macrophage; CHC, clathrin heavy chain; CNM, centronuclear myopathy; CPZ, chlorpromazine; CTL, control; Ctsk, cathepsin K; DKO, double knockout; M-CSF, macrophage colony stimulating factor; MDC, monodansylcadaverine; MNC, multinucleated cell; NFATc1, nuclear factor of activated T cells cytoplasmic 1; OCP, osteoclast precursor; PH, pleckstrin homology; PRD, proline-rich domain; RANKL, receptor activator of NF-κB ligand; TRAP, tartrate-resistant acid phosphatase.

The Rockefeller University Press $30.00
J. Cell Biol. Vol. 207 No. 1 73–89
www.jcb.org/cgi/doi/10.1083/jcb.201401137

Oikawa et al., 2012) have been suggested to contribute to fusion through the formation of these actin-rich structures.

We have previously shown that dynamin, a large GTPase best known for its function in the fission of vesicles from the plasma membrane during endocytosis (Hinshaw and Schmid, 1995; Takei et al., 1995; Ferguson and De Camilli, 2012), also participates in the regulation of actin remodeling in podosomes. In the process of vesicle fission, dynamin is thought to form a helical coil that constricts the neck of clathrin-coated pits, physically separating the budding vesicle from the plasma membrane (for review see Ferguson and De Camilli, 2012). In podosomes, dynamin is involved in actin reorganization through interactions with a large number of actin- and membrane-binding proteins that include profilin, cortactin, Abp1, proteins of the BAR domains superfamily (Witke et al., 1998; McNiven et al., 2000; Kessels et al., 2001; Itoh et al., 2005), and signaling proteins such as Src, Pyk2, and Cbl (Ochoa et al., 2000; Baldassarre et al., 2003; Bruzzaniti et al., 2005, 2009; Destaing et al., 2013). The two functions may be at least partially related, as actin is also found at clathrin-coated endocytic pits (Cao et al., 2003; Krueger et al., 2003; Ferguson et al., 2009; Grassart et al., 2014), where its assembly precedes the recruitment of dynamin (Ferguson et al., 2009; Taylor et al., 2012). Among the three dynamin isoforms encoded by mammalian genomes, dynamin 2 is ubiquitously expressed, and the mice in which dynamin 2 has been deleted in the germline die in early embryonic development (Ferguson et al., 2009). In osteoclasts, dynamin 2 is the predominant isoform (dynamin 1 is expressed at low levels, whereas dynamin 3 is undetectable) and dynamin GTPase activity modulates the dynamic organization of podosomes and bone resorption (Ochoa et al., 2000; Bruzzaniti et al., 2005).

Osteoclasts are multinucleated cells whose function is to resorb bone. They are formed by the asynchronous fusion of OCPs within the monocyte–macrophage lineage, and efficient bone resorption requires multinucleation. Based on the important role of dynamin in regulating both podosome formation and membrane remodeling as well as a recent report showing that dynamin is required in a post-membrane mixing stage before syncytia formation in primary myoblasts (Leikina et al., 2013), we hypothesized that dynamin might also play a role in the fusion of OCPs and thus represent a conserved component of the cell fusion–mediating machinery. To test this hypothesis, we used an inducible knockout mouse model to generate dynamin 1– and 2–deficient primary OCPs and myoblasts. Our results show that fusion of both cell types requires dynamin as well as endocytosis. At sites where cells are invaded by actin-rich protrusions from adjacent cells, high levels of clathrin-coated endocytic activity are observed. The formation of the actin protrusions and the localized endocytic activity are both impaired in the absence of dynamin, which is required in both fusing cells. Impairing endocytosis independently of dynamin by either depleting the cells of clathrin heavy chain (CHC), using pharmacological agents, or inhibiting the membrane recruitment of clathrin and the clathrin adaptor AP-2 also prevented cell–cell fusion. Collectively, these results indicate that cell–cell fusion involves dynamin and the formation of invadosome-like actin-rich protrusions associated with clathrin-mediated endocytosis. Since dynamin is involved in both the formation of invadosome-like actin-rich structures and in the endocytic process, our results indicate that dynamin function is central to the cell–cell fusion process of OCPs and myoblasts.

Results

Early OCPs express high levels of dynamin

Given that in osteoclasts dynamin is involved in the regulation of actin polymerization in podosomes and in bone resorption in vitro, and since actin-based structures and podosomes have been suggested to play a role in cell–cell fusion in myoblasts and in OCPs (Sens et al., 2010; Oikawa et al., 2012; Shilagardi et al., 2013), we focused on the potential role of dynamin in osteoclast fusion and differentiation using genetic tools to delete dynamins in early OCPs.

We first determined the time course of dynamin expression during early osteoclast differentiation in vitro. Dynamin protein levels increased markedly as early as 1 d after exposure to receptor activator of NF-kB ligand (RANKL; a cytokine required for OCP differentiation) and declined by day 3 (Fig. 1 A). The expression of CHC and of DC-STAMP, a molecule thought to be involved in OCP fusion, was also high at these early time points (Fig. 1 A). This increase was an immediate response to RANKL, occurring before the increase of the levels of osteoclast differentiation markers such as Src, cathepsin K, and the β3 integrin, whose expression is up-regulated by the osteoclastogenic transcription factor nuclear factor of activated T cells cytoplasmic 1 (NFATc1; Takayanagi et al., 2002; Kim et al., 2008; Zhao et al., 2010), and started to increase at day 2, peaking at day 3, a time at which both dynamin and DC-STAMP have already markedly decreased (Fig.1 A). Thus, dynamin expression is induced together with DC-STAMP in early mononuclear fusion-competent (Oursler, 2010) OCPs before the expression of classical osteoclast markers and at the time of active cell–cell fusion.

Deletion of dynamin 1 and 2 impairs the fusion of OCPs

To identify the role of dynamin in OCPs, we used cells derived from the Cre-ERT;*Dnm1*$^{fl/fl}$;*Dnm2*$^{fl/fl}$ mice in which both dynamin 1 and 2 genes are floxed and the Cre recombinase activity is inducible by 4-hydroxytamoxifen (4OHT) treatment (Ferguson et al., 2009) for all our in vitro studies. Conditional double deletion of dynamin 1 and 2 was selected for our studies because both isoforms are expressed in osteoclasts (although dynamin 2 predominates) and global deletion of dynamin 2 is embryonic lethal (Ferguson et al., 2009). Indeed, preliminary studies showed that deletion of dynamin 1 alone had only mild effects on these cells (unpublished data). This strategy allowed us to delete both isoforms and overcome redundant functions of these two closely related dynamins or the use of unspecific pharmacological inhibitors such as dynasore or dynGo (Park et al., 2013).

Deletion of the dynamin genes in OCPs was induced in vitro by treating bone marrow macrophages (BMMs) isolated from Cre-ERT;*Dnm1*$^{fl/fl}$;*Dnm2*$^{fl/fl}$ mice with 4OHT (*Dnm*-DKO), before induction of osteoclast differentiation. To control for the possible

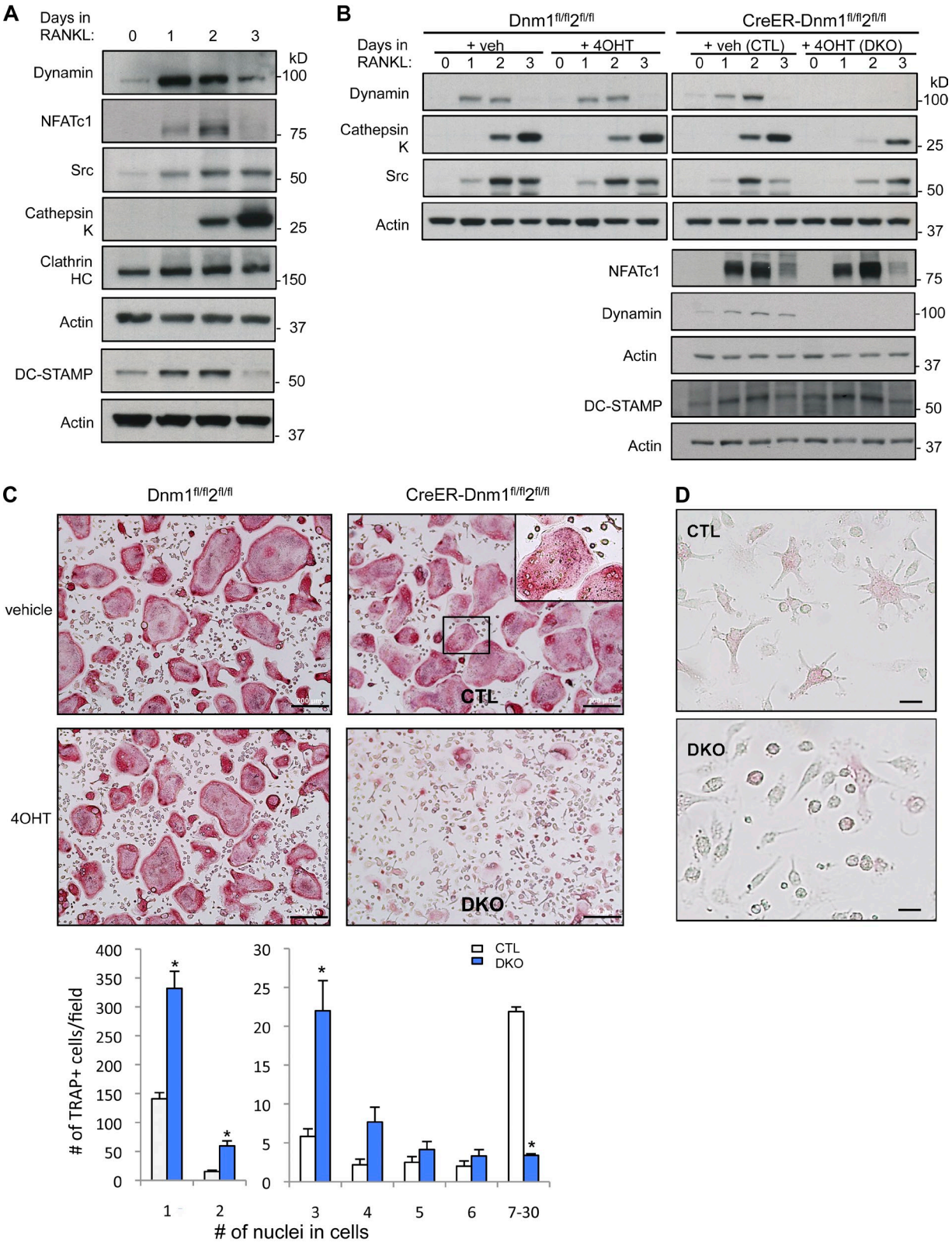

Figure 1. **Dynamin expression increases in early OCPs, and dynamin depletion impairs osteoclast multinucleation.** (A) Western blot analysis of BMM cell lysates stimulated with RANKL for the indicated days to evaluate expression levels of dynamin, NFATc1, Src, cathepsin K, CHC, and actin (loading control) during RANKL-induced osteoclast differentiation. (B) Western blot analysis of osteoclasts with the indicated antibodies and time points. Cells from littermate control mice *Dnm1*$^{flox/flox}$;*Dnm2*$^{flox/flox}$ were used as a control for tamoxifen treatment. (C) Representative images of TRAP-stained osteoclasts differentiated from bone marrow of *Dnm1*$^{flox/flox}$;*Dnm2*$^{flox/flox}$ mice and CreER;*Dnm1*$^{flox/flox}$;*Dnm2*$^{flox/flox}$ littermates. Osteoclast multinucleation was quantified by counting the number of TRAP+ cells with one to two nuclei (left) or three or more nuclei (right). The inset is an enlarged view of the boxed region. Data are means ± SD (error bars) from five independent experiments. *, $P < 0.001$. Bars, 200 µm. (D) Images of TRAP-stained CTL and DKO osteoclasts after culturing with RANKL for 1 d. Note that DKO cells are round and have less prominent filopodia, compared to CTL cells. Bars, 10 µm.

effect of 4OHT, BMMs derived from *Dnm1*$^{fl/fl}$;*Dnm2*$^{fl/fl}$ mice were treated with the same concentration of 4OHT. Dynamins were efficiently depleted in *Dnm*-DKO cells as determined by Western blotting with anti-dynamin antibodies recognizing both dynamin 1 and 2 (Fig. 1 B).

Strikingly, whereas the induction of the RANKL target gene and master osteoclastogenic transcription factor NFATc1 was unaffected by deletion of dynamin (Fig. 1 B), demonstrating that RANK signal transduction is not affected by the absence of dynamin, the number of multinucleated cells positive for the osteoclast marker enzyme tartrate-resistant acid phosphatase (TRAP; TRAP+ multinucleated cells [MNCs]) formed in vitro in the presence of macrophage colony stimulating factor (M-CSF), and RANKL was markedly reduced in the *Dnm*-DKO cells (Fig. 1 C). The number of OCPs that remained mononuclear in these cultures was about threefold higher than in control cultures. The fact that small osteoclasts with few nuclei were predominant in double knockout (DKO) cultures may be due to some fusion occurring in this assay before the addition of 4OHT or to only partial deletion of Dnm1,2. It is also possible that some impairment of cytokinesis (Liu et al., 2008) generated some of the cells with two to three nuclei, decreasing the apparent effect of Dnm1,2 deletion on OCP fusion. These results demonstrate that dynamin is required for the OCPs to efficiently form multinucleated cells through cell–cell fusion, despite the fact that, like NFATc1, the expression of DC-STAMP was not affected by dynamin deletion (Fig. 1 B). Although expression of NFATc1 was intact, the expression of several of its target genes and markers of mature osteoclasts, including Src and cathepsin K (Ctsk), was delayed in the *Dnm*-DKO cells (Fig.1 B), which suggests that impairing the fusion of OCPs may affect the subsequent differentiation of osteoclasts. Furthermore, the cell morphology was significantly altered in the absence of dynamin. Control OCPs had a stellar or spindle-shaped morphology with numerous protrusions, whereas *Dnm*-DKO cells exhibited a rounded and flattened appearance with fewer and shorter extensions (Figs. 1 D and 6 A).

Perturbation of dynamin function affects actin polymerization and cell migration (McNiven et al., 2000; Ochoa et al., 2000; Kawada et al., 2009; Destaing et al., 2013), and indeed, cell migration was significantly decreased (by 25–30%, $P < 0.001$) in *Dnm*-DKO OCPs (Fig. S1 A). Since OCPs must migrate and meet in order to fuse and form multinucleated cells, we then determined whether the fusion defect could be due to impaired migration, independent of the cell–cell fusion process itself. For this purpose, we plated OCPs at increasingly higher densities to compensate for their defective migration. As expected, multinucleation of control cells increased with increasing OCP plating density. In contrast, increasing cell density even up to the point of providing direct cell–cell contact failed to rescue the cell–cell fusion defect of *Dnm*-DKO cells (Fig. 2 A). These data demonstrate that dynamin is required for OCP cell–cell fusion, independent of the establishment of cell–cell contacts.

To test this hypothesis further, we cocultured equal numbers of OCPs whose membranes were labeled with either of the lipophilic dyes DiI (red) or DiO (green) in the presence of M-CSF and RANKL, and determined the percentage of fused cells (yellow/orange; Fig. 2 B). Dynamin depletion resulted in a markedly decreased OCP fusion efficiency (Fig. 2, C and D), with most of the cells having only two to three nuclei (see Fig. 1 C). Using a membrane dye (DiI) and a cytoplasmic marker (CellTracker), we further confirmed that the efficiency of multinucleation (syncytium formation) is markedly impaired (>80%, $P < 0.01$) in the absence of Dnm1/2. These results show that dynamin is required for efficient fusion of OCPs. In contrast, the number of mononuclear cells showing evidence for prior occurrence of a lipid-mixing event (mononuclear yellow cells, Fig. 2 D) or partial lipid-content mixing (mononuclear yellow cells, Fig. 2 F) was not significantly affected (Fig. 2 F) or even slightly decreased (Fig. 2 D) by the deletion of dynamin 1 and 2 when it should have increased if the fusion impairment was posterior to the early mixing of membranes or content. These observations suggest that early lipid mixing or content mixing events may also decrease in the absence of dynamin.

We then determined whether dynamin was required in both partners of the OCP cell–cell fusion event by mixing control (CTL) and DKO cells in the same culture and measuring syncytium formation and lipid mixing efficiency. Interestingly, we observed a similar reduction (>80%, $P < 0.01$) in syncytium formation and in the level of lipid mixing as observed with DKO cells, which indicates that dynamin is required in both cell fusion partners (Fig. 2, E and F).

Consistent with the reduced number of TRAP+ MNCs formed in these cultures, the resorbed surface generated by *Dnm*-DKO OCs plated on dentine slices was also reduced by ∼80% ($P < 0.05$, Fig. 3 A). Accordingly, conditional KO mice (*Dnm*-DKO;Ctsk) generated by crossing osteoclast-specific Ctsk-Cre mice (Nakamura et al., 2007) with *Dnm1*$^{fl/fl}$;*Dnm2*$^{fl/fl}$ mice (Ferguson et al., 2009) and in which dynamin protein level was decreased by 40–50% and 50–60% at days 1 and 2, respectively, in *Dnm*-DKO;Ctsk cells (Fig. S1 B) showed a significant decrease (by ∼15%, $P < 0.01$) in serum levels of cross-linked C-telopeptide of type I collagen (CTX), a marker of osteoclast activity. This indicates that bone resorption is globally decreased in *Dnm*-DKO;Ctsk mice (Fig. 3 B). This resulted in an increased bone mass in vivo as shown by micro-CT (µCT; Fig. 3, C and D) and histomorphometric analysis (Fig. 3, E and F). Most relevant to this study is the markedly decreased number and size of osteoclasts (Fig.3 F), demonstrating that deletion of dynamin affected both the differentiation and size of osteoclasts in vivo. The increase in bone volume is only moderate however, most likely due to the fact that Ctsk promoter-driven Cre expression occurs later than the initiation of OCP fusion (see Fig. 1 A). Osteoclast size was still affected given that fusion continues to proceed during the lifetime of osteoclasts (Fig. 1, A and B; and Fig. S1 B). These results establish the fact that our observations on the role of dynamin in osteoclasts differentiation and function also apply to the in vivo situation.

The pleckstrin homology (PH) and proline-rich domain (PRD) of dynamin are required for OCP fusion

Dynamin comprises several functional domains. The dynamin PH domain binds to acidic phospholipids on the cytosolic side

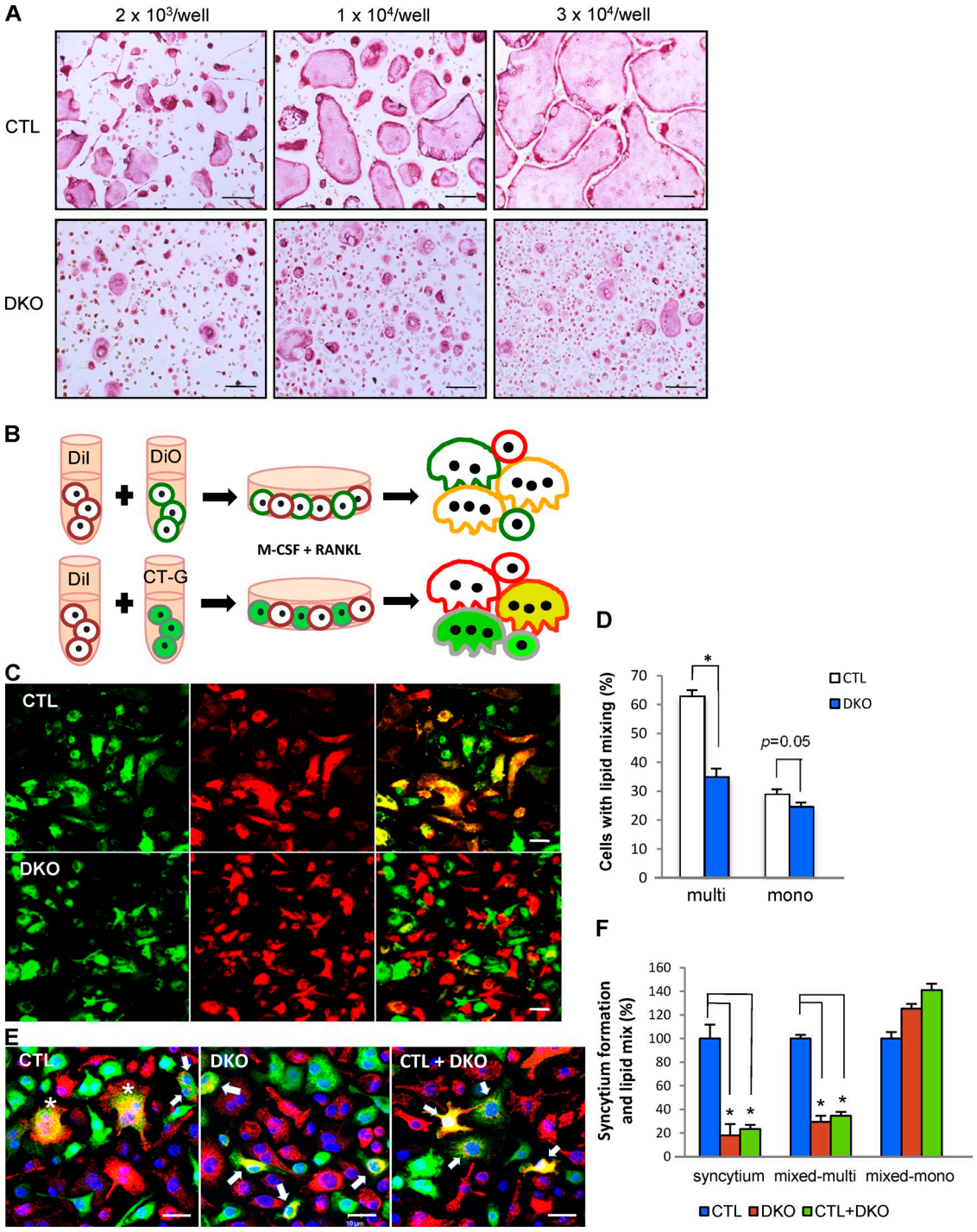

Figure 2. **Dynamin depletion reduces osteoclast fusion independently of cell migration.** (A) OCPs were plated at three different densities as indicated, and differentiation was induced by M-CSF and RANKL for 3 d. Images are representative of results from three independent experiments carried out in triplicate. Bar, 20 µm. (B) Cell fusion scheme for lipid mix and for content mixing assays for experiments described in C and E. CTL and DKO OCPs were generated as described in the Materials and methods: separated in two pools, labeled with membrane probes DiI (red) and DiO (green), or DiI and cytoplasmic probe CellTracker Green (CT-G), and cultured together in the presence of M-CSF and RANKL for 3–4 d. (C) Representative images of the cells labeled with DiI (red) or DiO (green) and fused as described in B. Bars, 20 µm. (D) The percentages of multinuclear (three or more nuclei) and mononuclear yellow cells (lipid mix) from assays as in C were determined. Data are mean ± SE (error bars); *, $P < 0.01$). (E) Images of the cells labeled with membrane probe DiI (red), green CellTracker, and DAPI (blue). Arrows and asterisks indicate colabeled mononuclear cells and multinuclear cells, respectively. Bars, 20 µm. (F) Quantification of syncytium formation and lipid and content mixing in CTL, DKO, and a mix of CTL and DKO cultures as in E. Data were normalized to those of CTL cells. All data are means ± standard error (error bars; $n \geq 3$). *, $P < 0.01$.

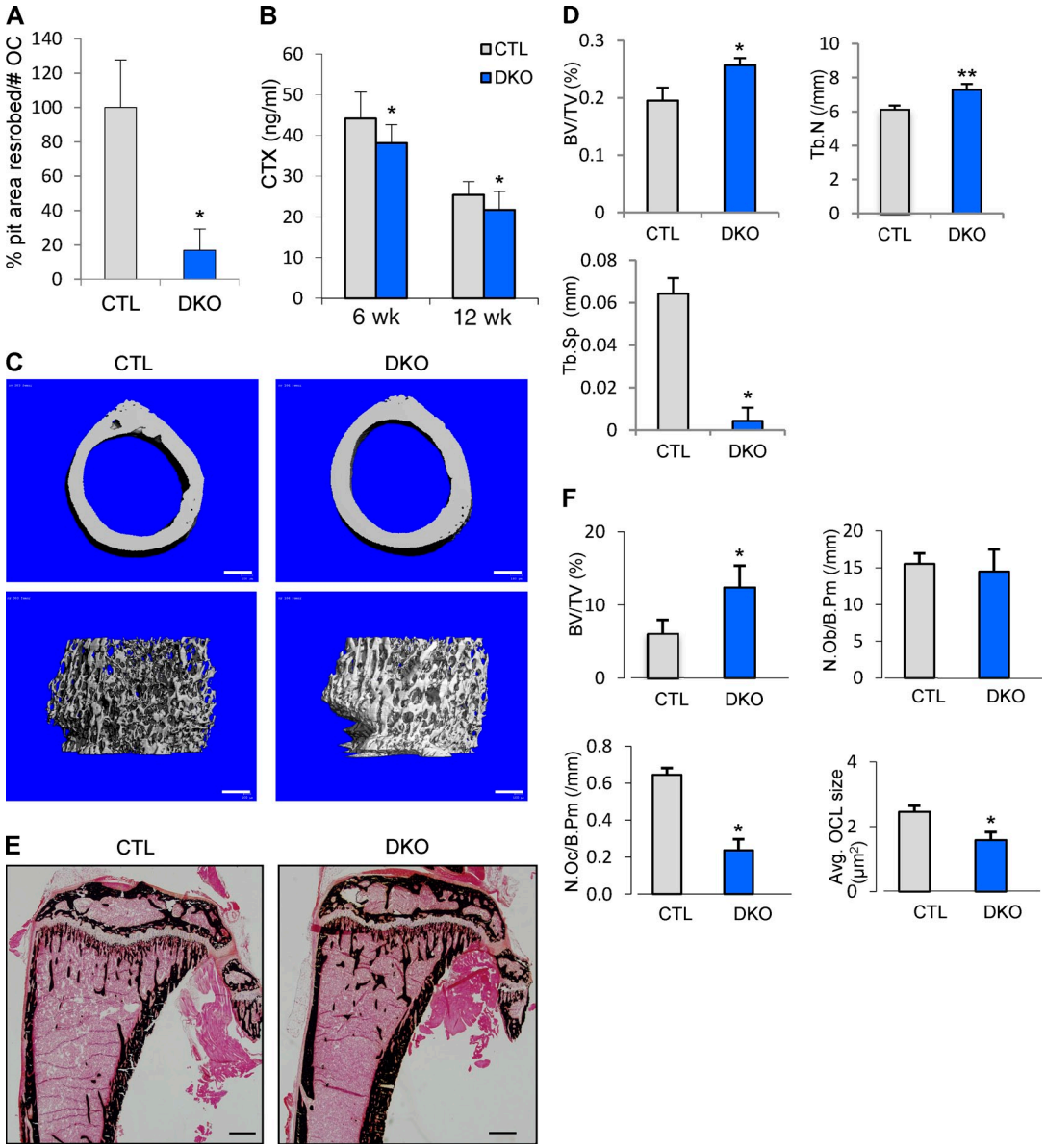

Figure 3. **Osteoclast-targeted conditional dynamin deletion in mice decreases osteoclast numbers, size, and bone resorption, resulting in higher bone mass.** (A) Resorption pits were formed by CTL and *Dnm*-DKO;ERT osteoclasts (OCs) cultured on dentin slices. The resorbed areas were measured and normalized to the number of osteoclasts on dentin slices. The values are mean ± SD (error bars) of triplicates; dynamin-depleted osteoclasts formed less resorption pits ($P < 0.05$). (B) Serum CTX levels of 6-wk-old CTL and *Dnm*-DKO;Ctsk (DKO) mice ($n = 5$). Data are means ± SD (error bars). *, in vivo bone resorption was lower in DKO mice ($P < 0.01$). (C) Representative µCT images of femurs from CTL and *Dnm*-DKO;Ctsk (DKO) mice at 6 wk. Bars, 200 µm. (D) µCT analysis of distal femur of CTL and *Dnm*-DKO;Ctsk (DKO) mice. Results are mean ± SE (error bars; female, $n = 4$). *, $P < 0.05$; **, $P < 0.01$. BV/TV, trabecular bone volume (% bone volume); Tb.N, trabecular number; Tb.Sp, trabecular spacing. (E) Von Kossa staining of tibia sections from 6-wk-old *Dnm*-DKO;Ctsk (DKO) mice and littermate controls (CTL) showing increased bone mass. Bars, 400 µm. (F) Histomorphometric analysis of tibia samples ($n = 5$). BV/TV, trabecular bone volume (% bone volume); N.Ob, number of osteoblasts; N.Oc, number of osteoclasts. All data are means ± SD (error bars). *, $P < 0.05$.

of the plasma membrane (Ferguson et al., 1994; Zheng et al., 1996), and a defective PH domain inhibits clathrin-mediated endocytosis (Lee et al., 1999; Vallis et al., 1999). The PRD interacts with SH3 domain–containing proteins, including several actin-regulatory proteins, and contributes to the localization of dynamin at endocytic sites and to the coordination of dynamin function during endocytosis (Ferguson and De Camilli, 2012). Accordingly, dynamin lacking the PRD cannot rescue endocytic defects in dynamin-knockout fibroblasts (Ferguson et al., 2009). Lastly, the GTPase domain is responsible for GTP binding and hydrolysis. To determine the functional role of each of these domains in the OCP fusion process, we performed rescue experiments in DKO OCPs using lentiviral constructs of dynamin 2 (Dnm2) WT or Dnm2 mutants including a deletion of the PRD domain (ΔPRD), a mutation of the PH domain (K562E), or a mutation in the GTPase domain (K44A), as well as dynamin 1 (Dnm1) WT or an empty vector. Whereas Dnm2 WT efficiently rescued the defective fusion phenotype of Dnm-DKO OCPs ($P < 0.001$), Dnm1 rescued ($P < 0.01$) significantly less than Dnm2 ($P < 0.03$ vs. Dnm2). In contrast, the mutants Dnm2-K562E and Dnm2-ΔPRD or Dnm2-K44A failed to rescue fusion in this assay (Fig. 4). These results are consistent with the need for

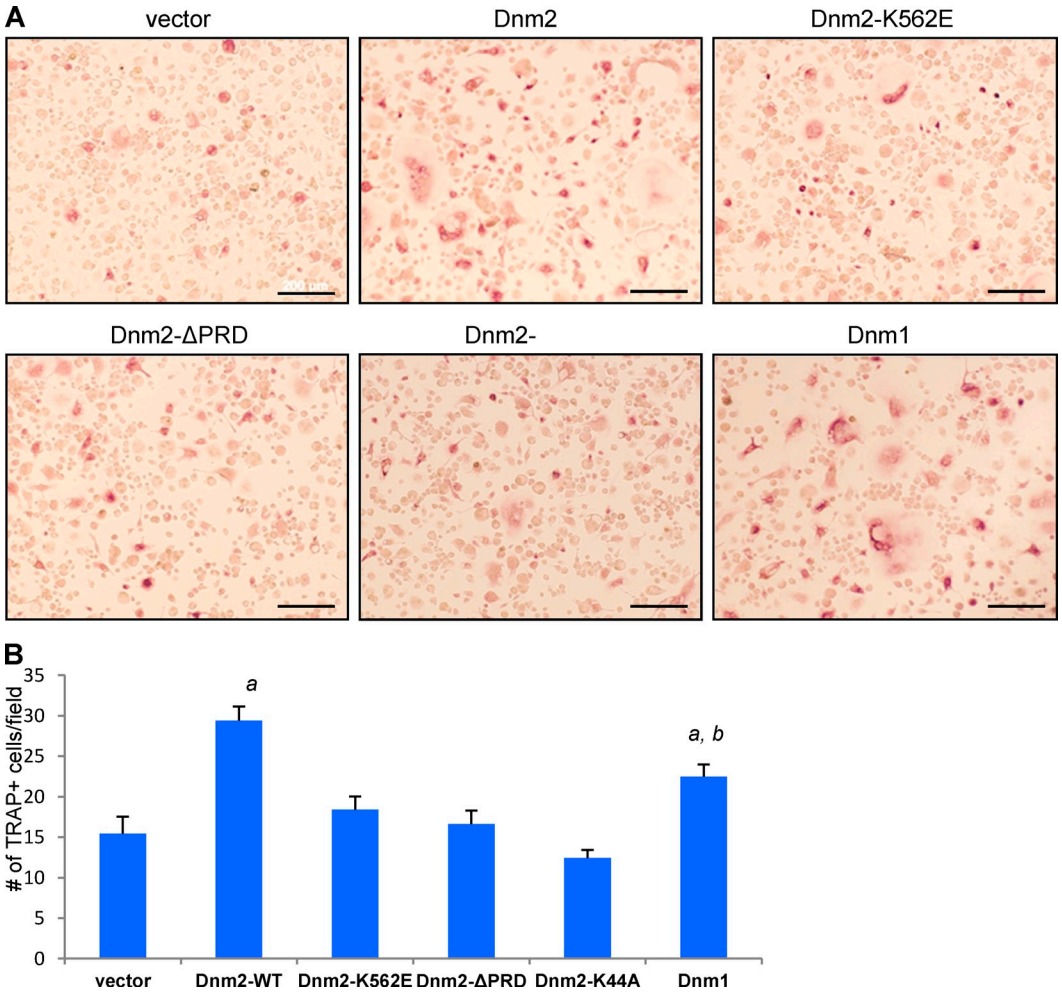

Figure 4. **Dynamin PRD and PH domains are required for the fusion of OCPs.** (A) TRAP staining of transduced *Dnm*-DKO osteoclasts reexpressing vector, dynamin 1 (Dnm1), dynamin 2 (Dnm2) WT, and Dnm2 mutants including a GTPase mutant K44A, a PH domain mutant K562E, and a splice variant ΔPRD. Bars, 200 µm. (B) Quantification of TRAP-positive cells with more than three nuclei for fusion rescue efficiency. One-way ANOVA ($P < 0.001$) and a Student's *t* test were used to analyze the data. *a*, significantly different from vector ($P < 0.001$); *b*, significantly different from Dnm2 ($P < 0.034$).

protein interactions of the PRD or PH domains as well as for the GTPase activity (also supported by the effect of dynasore on OCP fusion; Fig. S3) for the actions of dynamin in OCPs fusion (Fig. 4). Thus, the entire dynamin function appears to be required for OCP cell–cell fusion.

Dynamin deletion alters the formation of actin-rich membrane protrusions at the time of OCP fusion

Dynamin is highly enriched in the podosome belt of mature osteoclasts and regulates podosome organization and dynamics (Ochoa et al., 2000; Bruzzaniti et al., 2005; Destaing et al., 2013). Podosomes or podosome-like structures have recently been shown to be associated with the fusion of myoblasts and of OCPs (Sens et al., 2010; Oikawa et al., 2012). We therefore examined the behavior of podosomes during OCP fusion in the presence or absence of dynamin. Time-lapse imaging of live osteoclasts expressing GFP-actin and differentiating in the presence of RANKL and M-CSF showed that small clusters of podosomes often appeared at the contact areas between fusing cells (Fig. S2), as recently observed by Oikawa et al. (2012).

Confocal microscopy confirmed that dynamin is highly enriched in mononuclear OCPs and expressed at lower levels once the cells become multinucleated (Fig. 5 A), in agreement with our qPCR (not depicted) and Western blot data (Fig. 1, A and B). Indeed, fusion-competent OCPs stimulated by RANKL could be distinguished on the basis of their high level of expression of dynamin, CHC, and DC-STAMP as early as 1 d after exposure (Fig. 5, B and C; and Fig. 6, B and C).

In addition to these podosome-like structures, confocal analysis of OCPs at day 1 and 2, a time of active fusion, showed a prominence of markedly elongated dynamin- and F-actin–rich structures protruding from the OCPs and often into the apposing cell at sites of cell–cell contact (Fig. 5 D, boxed area). These structures were also identifiable between day 2 and 3 after exposure to RANKL, when mononuclear or binucleated OCPs fused with already established MNCs. Interestingly, DC-STAMP was also enriched in these early precursors, where it partially colocalized with CHC (Fig. 5 E). At the time of increased cell fusion, DC-STAMP was found in actin-rich protrusions of OCPs (Fig. 6 B) and/or in the membrane of the apposed cell (Fig. 6 C). In contrast,

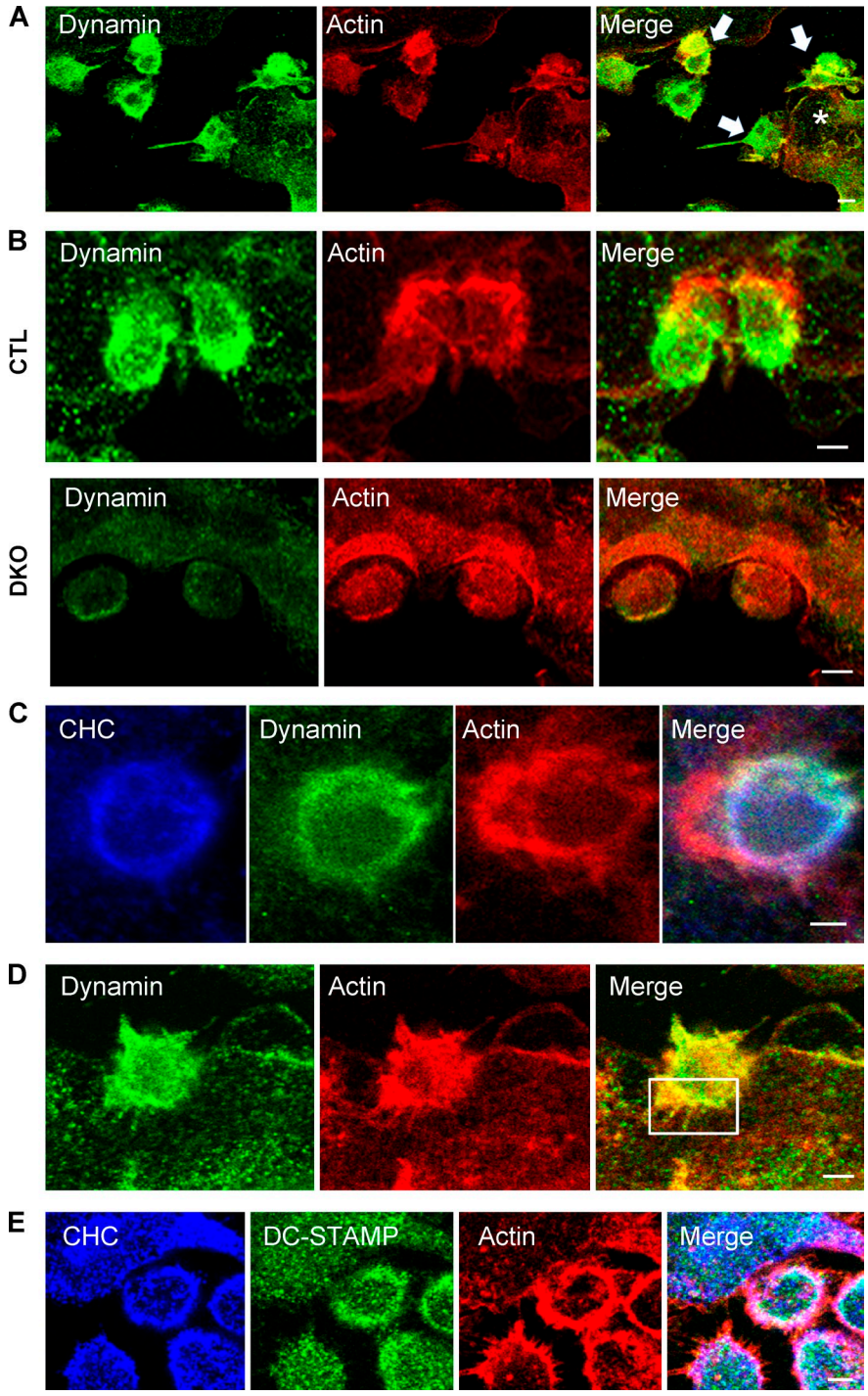

Figure 5. **OCPs express high levels of dynamin and DC-STAMP, and form actin-rich structures at the time of fusion.** Immunofluorescence confocal images of OCs in fusion stained with antibodies to dynamin, CHC, DC-STAMP, and rhodamine-phalloidin for F-actin labeling. (A) Dynamin-enriched OCPs (arrows) fusing with an already multinucleated osteoclasts (OCL; asterisk) in which dynamin levels are low. (B) Dynamin and actin are highly enriched in fusing CTL cells, whereas dynamin expression is markedly suppressed in DKO cells (note that dynamin expression was markedly suppressed). (C) Accumulation of actin at sites of cell–cell fusion in both the recipient and the fusing cell, where CHC, dynamin, and actin are colocalized. (D) Note the prominent filopodia (box) enriched with dynamin and actin protruding from a mononuclear cell fusing into a larger multinuclear cell. (E) CHC and DC-STAMP are also enriched and colocalized in mononuclear OCPs. Bars, 5 µm.

Dnm-DKO OCPs exhibited markedly fewer and shorter actin-rich protrusions in general and at sites of cell–cell contacts (Fig. 6, A and B).

Importantly, actin, clathrin, dynamin, and DC-STAMP were also enriched at sites of fusion in the apposing cell (Fig. 5, C and E; and Fig. 6 C), which confirms our observation that dynamin is required in both fusing cells (Fig 2, E and F) and suggests that the invaded cell's actin and clathrin machinery might also be involved in the invasion process, which is reminiscent, except for DC-STAMP, of what is observed during the invasion of cells by *Listeria* (Bonazzi et al., 2011).

Ultrastructural analysis of fusion sites by transmission electron microscopy confirmed and extended these observations. In control cells, as with confocal analysis, we frequently observed multiple finger-like actin-rich protrusions (Fig. 6 A) extending into the apposing cells, confirming the confocal observations (see Fig. 5, A and D). These protrusions are highly reminiscent of invadosomes and of the invasive structures seen in fusing myoblasts in *Drosophila melanogaster* (Kesper et al., 2007; Berger et al., 2008; Sens et al., 2010). These protrusive structures had a mean length of 2 µm and a diameter of about 180 nm, and were enriched with packed and longitudinally

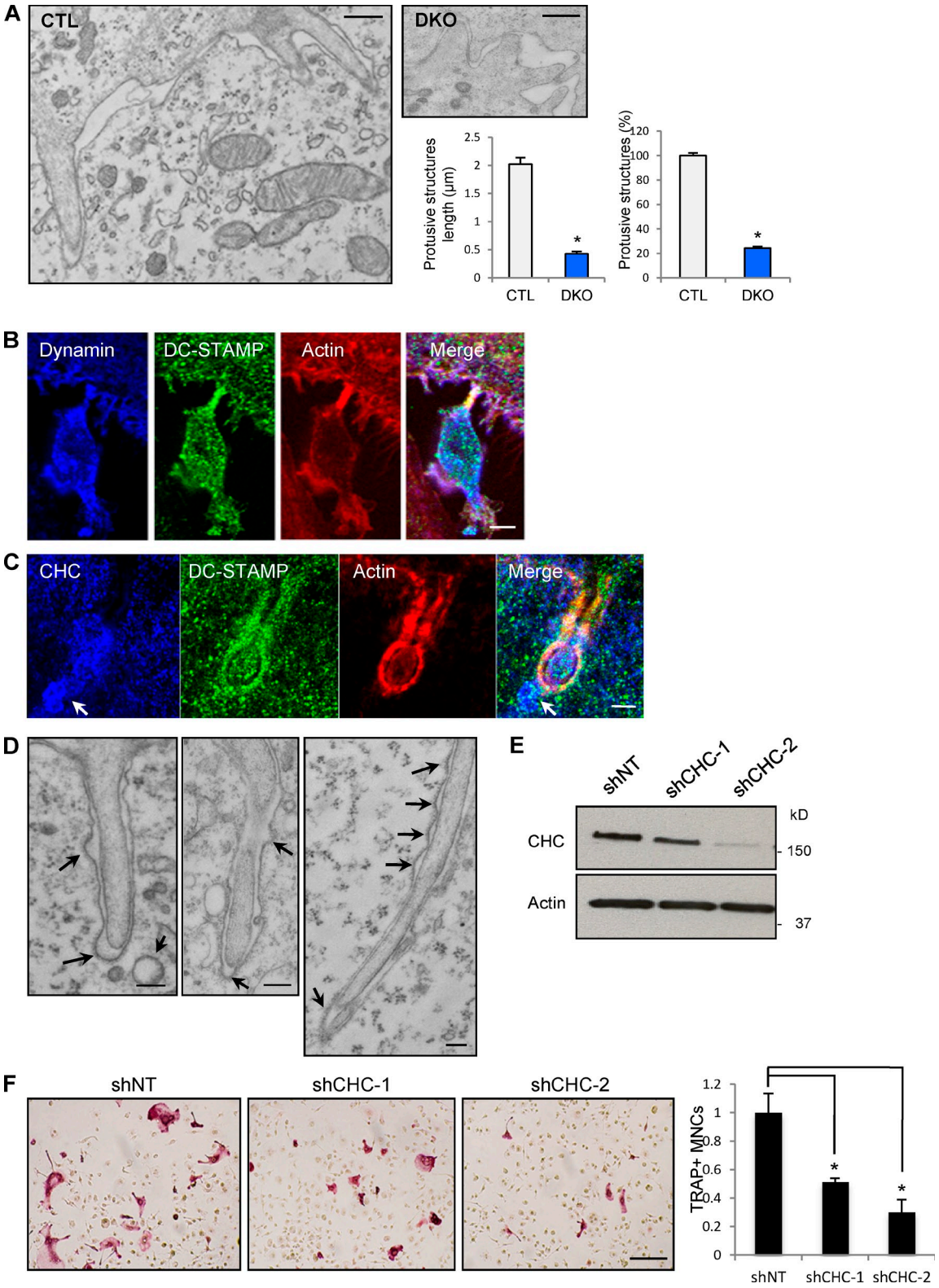

Figure 6. **Dynamin-dependent actin-rich protrusions are associated with clathrin-coated vesicles at sites of OCP fusion.** (A) Electron microscopy images of representative OCPs showing F-actin–rich membrane protrusions extending from one cell into the adjacent cell, similar to confocal images in Fig. 5 D of CTL cells. Bars, 200 nm. The length of protrusive structures of CTL osteoclasts (OCLs) is about five times longer than those of DKO cells (left graph, $P < 0.01$). The number of protrusive structures was 80% less in DKO cells ($P < 0.01$). Data were obtained from 38 CTL and 86 DKO cell images in three independent experiments. Error bars indicate SEM. (B) Colocalization of dynamin and DC-STAMP on an OCP actin protrusion. Bar, 5 μm. (C) The localization of CHC and DC-STAMP around and at tips of the protrusions of osteoclasts in CTL culture; note the presence of clathrin-coated vesicles near the tip of the protrusion (arrows). Bar, 0.3 μm. (D) EM images showing the frequent association of F-actin protrusions and clathrin-coated pits (arrows) in the membrane of the invaded cells. Bars, 200 nm. (E and F) shRNA-mediated knockdown of CHC was analyzed by Western blotting. TRAP-positive multinucleated osteoclasts were quantified. Data are mean ± SE (error bars). *, $P < 0.01$. Bar, 200 μm.

oriented actin filaments (Fig. 6 A). In contrast, the *Dnm*-DKO cells formed ∼80% less ($P < 0.01$) protrusive structures, and these were 80% shorter ($P < 0.01$), most often without prominent accumulation of actin filaments bundles (Figs. 5 B and 6 A), which suggests that formation and/or extension of these protrusions is dynamin dependent. Thus, the confocal and EM analyses suggest that dynamin contributes to the formation of protrusive actin-rich structures that are associated with the fusion of OCPs, whereas the fusion assays demonstrate that fusion is impaired in the absence of dynamin. The actin-based function of dynamin may therefore contribute to the efficient cell–cell fusion of OCPs.

Quite strikingly, our EM studies showed not only that fusing OCPs generated long actin-rich invasive membrane protrusions (Fig. 6 D) but also that these were frequently associated with the presence of clathrin-coated pits in the apposed recipient cell membranes, often located opposite to the tips of the protrusion (Fig. 6, C and D, arrows; 20 clathrin-coated pits around the cross-section of 38 protrusions, 9 of which were opposite to the tips).

These observations suggest a role for both the invading and the invaded cell in the fusion process, as demonstrated by the fact that dynamin is required in both OCPs during the fusion process (Fig. 2, E and F). We also often observed coated vesicles in the vicinity of the protrusions (Fig. 6, A and D).

These observations suggested the possibility that both the dynamin-dependent actin-based mechanisms and the endocytic activity at sites where cell contact is established by these protrusions could be involved in the fusion process of OCPs.

Endocytosis is also required for the fusion of OCPs

Dynamin deletion blocks clathrin-mediated endocytosis in *Dnm*-DKO fibroblasts (Ferguson et al., 2009) and results in a striking accumulation of highly tubulated endocytic pits on the plasma membrane. Accordingly, analysis of confocal microscopy z sections revealed a higher abundance of endocytic pits labeled with CHC, endophilin, or DC-STAMP (approximately twofold, $P < 0.01$; Fig. S3 A) at the plasma membrane of the *Dnm*-DKO OCPs, as well as decreased intracellular localization of DC-STAMP (by ∼60%, $P < 0.01$; Fig. S3 A) that, in early OCPs, colocalizes partially with CHC (see Fig. 5 E).

To determine whether alterations in endocytosis, also a consequence of dynamin depletion, contributed to the impaired OCP cell–cell fusion, we then explored whether perturbations of clathrin-mediated endocytosis by means other than deletion of dynamin would alter OCP fusion in vitro. For this purpose, we targeted the machinery involved in clathrin-mediated endocytosis by knocking down CHC by lentiviral shRNA transduction of BMMs. This resulted in a >90% decrease in the expression of CHC and markedly decreased OCP fusion (Fig. 6 E). This finding was also confirmed by treatment of OCPs with chlorpromazine (CPZ), which is known to affect hemifusion intermediates (Chernomordik et al., 1999), or monodansylcadaverine (MDC), two drugs that have an inhibitory effect, although not entirely specific, on clathrin-mediated endocytosis and that also blocked OCP fusion in vitro (Fig. S3 B).

Collectively these results show that dynamin function and clathrin-mediated endocytosis, which appears to be highly enhanced at sites of cell–cell contacts, are required, directly or indirectly, for the proper fusion of OCPs.

Dynamin and endocytosis also play a role in myoblast fusion

We then asked whether these observations were specific to OCPs or if they could be extended to the fusion of another cell type, the myoblast. A role for dynamin in myoblast fusion has recently been suggested in vitro using dynasore and shRNA transfection in the C2C12 cell line and primary myoblasts (Leikina et al., 2013). Protein levels of dynamin 2 mildly increased, whereas dynamin 1 decreased during myoblast differentiation (Fig. S4 A). Levels of dynamin 3, typically expressed at low levels (or absent) outside the brain (Ferguson et al., 2009), were low irrespective of the differentiation state of myoblasts.

Taking advantage of our double knockout in vivo system, we tested the role of dynamin in the fusion of primary myoblasts isolated from *Dnm*-DKO;ERT mice as we did in our OCP studies. When induced by serum withdrawal from the culture, myoblasts go through a series of developmental steps to form multinucleated myotubes. Interestingly, depletion of dynamin in primary myoblasts (*Dnm*-DKO) resulted in impaired fusion and a decrease of >60% ($P < 0.01$) in myotube formation (Fig. 7, A and B). This observation confirms a specific function for dynamin in the fusion event that is separable from the signaling events that drive myoblast differentiation, similar to our observations in OCPs.

We then used the model cell line C2C12 for studies of myoblast fusion to explore whether the importance of dynamin in cell fusion could reflect a role of clathrin-mediated endocytosis in this process. An efficient knockdown of the dynamin gene by shRNAs markedly reduced myotube formation in C2C12 myoblast differentiation culture (Fig. S4 B), confirming the results of Leikina et al (2013). Additionally, confocal and ultrastructural analyses showed that, as observed in OCPs and in *Drosophila* (Sens et al., 2010), fusing mammalian myoblasts also exhibited actin-rich protrusions (Fig. S4 C).

We next targeted clathrin-mediated endocytosis independently from dynamin by knocking down CHC by siRNA transfection. This markedly reduced the number of fused myotubes (Fig. 8 A). We also transfected C2C12 cells with the amphiphysin fragment A1, which prevents clathrin-mediated endocytosis by blocking the recruitment and thus assembly of clathrin (Slepnev et al., 1998, 2000). In A1-expressing cells, both transferrin uptake (a reporter of clathrin-mediated endocytosis) and cell fusion were impaired (Fig. 8 B). In contrast, in cells expressing an A1 mutant that cannot block clathrin interactions (Slepnev et al., 2000; A1/HSR/SR/SSR mutant), transferrin uptake and cell fusion were not impaired. Similar results were obtained with the pharmacological inhibitors CPZ and MDC, further establishing a role for endocytosis in myoblast fusion (Fig. S4 D).

These data demonstrate that dynamin function and endocytic events are also involved in myoblast fusion to form myotubes, as

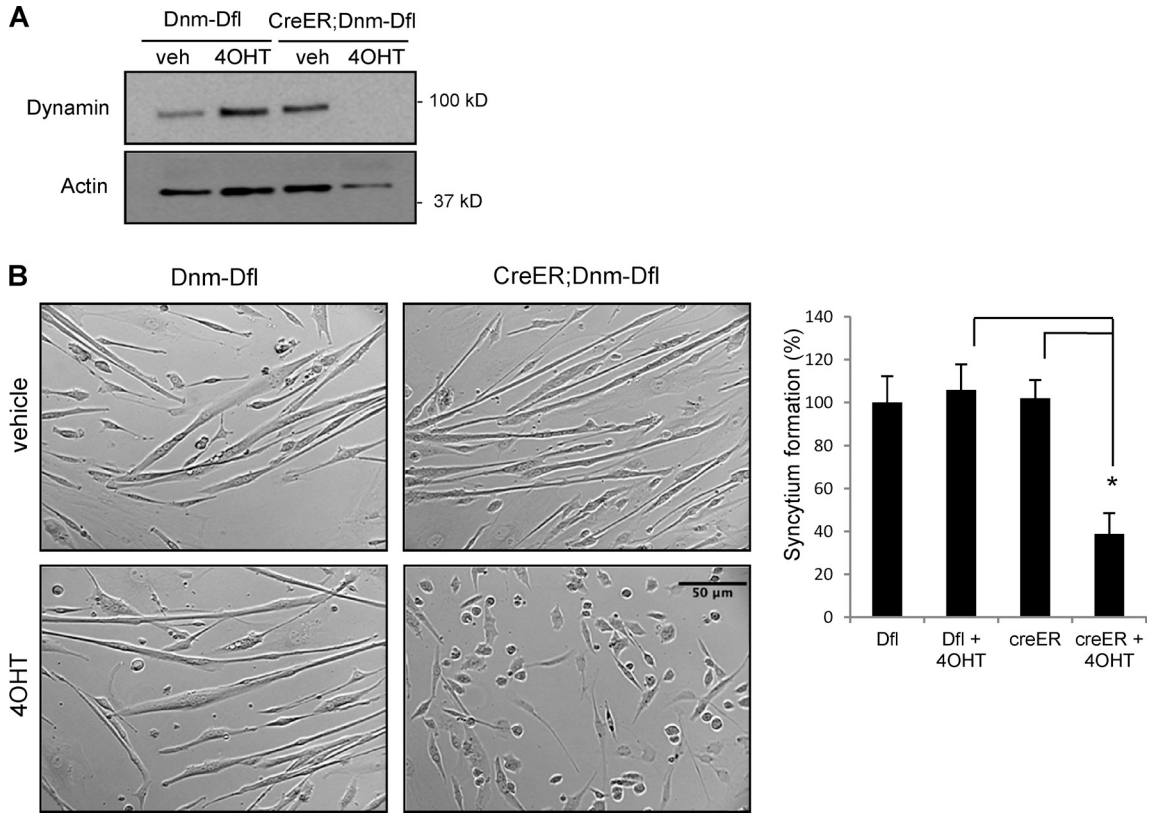

Figure 7. **Dynamin depletion also prevents primary myoblast fusion.** Primary myoblasts isolated from *Dnm1*$^{flox/flox}$;*Dnm2*$^{flox/flox}$ mice and CreER;*Dnm1*$^{flox/flox}$;*Dnm2*$^{flox/flox}$ littermates were cultured in differentiation medium for 4 d with or without 4OHT. (A) Dynamin depletion in creER;Dnm-Dfl cells after 4OHT treatment is shown by Western blot analysis. (B) DNM-DKO myoblasts showed a defect in myotube formation (phase-contrast microscopy), and the syncytium formation extent was quantified and normalized to Dfl cells. Error bars indicate SEM. *, P < 0.01.

they are in the fusion of OCPs to form osteoclasts, which suggests that dynamin and endocytosis dependence might be a general characteristic of cell–cell fusion.

Discussion

Our results demonstrate that deletion of dynamin 1 and 2 in OCPs and in myoblasts impairs the ability of these two cell types to undergo homotypic fusion to yield multinucleated osteoclasts or myotubes, respectively. Dynamin is involved in the regulation of actin polymerization at podosomes (Ochoa et al., 2000; Bruzzaniti et al., 2005, 2009) and at endocytic sites through direct and indirect interactions with actin-binding/regulating proteins, such as cortactin, profilin, Abp1, and Rac1 (McNiven et al., 2000; Kessels et al., 2001; Schafer et al., 2002; Schlunck et al., 2004; Pirraglia et al., 2006). The essential role of dynamin for the membrane fission reaction that separates endocytic clathrin-coated pits from the plasma membrane is also tightly interconnected with actin function (Ferguson and De Camilli, 2012; Taylor et al., 2012; Grassart et al., 2014). Here we show that long invadosome-like actin-rich protrusions are formed between fusing OCPs and fusing mammalian myoblasts, as previously reported in *Drosophila* (Sens et al., 2010; Shilagardi et al., 2013), and that deletion of dynamin 1 and 2 blunts the formation of these structures and prevents fusion of both OCPs and myoblasts, independent of its effects on cell migration. Importantly, these effects arising from dynamin depletion cannot be attributed to perturbations in RANK signaling and the ensuing expression of marker genes such as NFATc1 and DC-STAMP in OCPs or expression of MHC in myoblasts.

Furthermore, we show that the defective fusion in dynamin 1– and 2–deficient cells can be efficiently rescued in vitro by dynamin 2 and dynamin 1 (albeit less efficiently) but not by dynamin mutants in which the PRD, the PH, or the GTPase domains were deleted or mutated (Mooren et al., 2009; Ferguson and De Camilli, 2012). Such findings are consistent with structural studies (Damke et al., 1994; Chappie et al., 2011; Faelber et al., 2011; Ford et al., 2011; Destaing et al., 2013) that have established the integrated role of all the dynamin domains and dynamin oligomerization for its mechano-enzyme activity. They suggest that such activity of dynamin, which is required for endocytosis, is also required for the cell–cell fusion process. This is possibly because, as we show here, normal clathrin-mediated endocytosis is itself required for cell–cell fusion.

As it is not possible to separate the endocytic versus actin regulatory functions of dynamin, we tested whether inhibition of endocytosis would affect fusion independently of dynamin. Our results, obtained with specific depletion of CHC or prevention of clathrin-endocytic adaptor interactions via expression of a truncated amphiphysin (Slepnev et al., 2000), as well as with broad action pharmacological inhibitors of endocytosis,

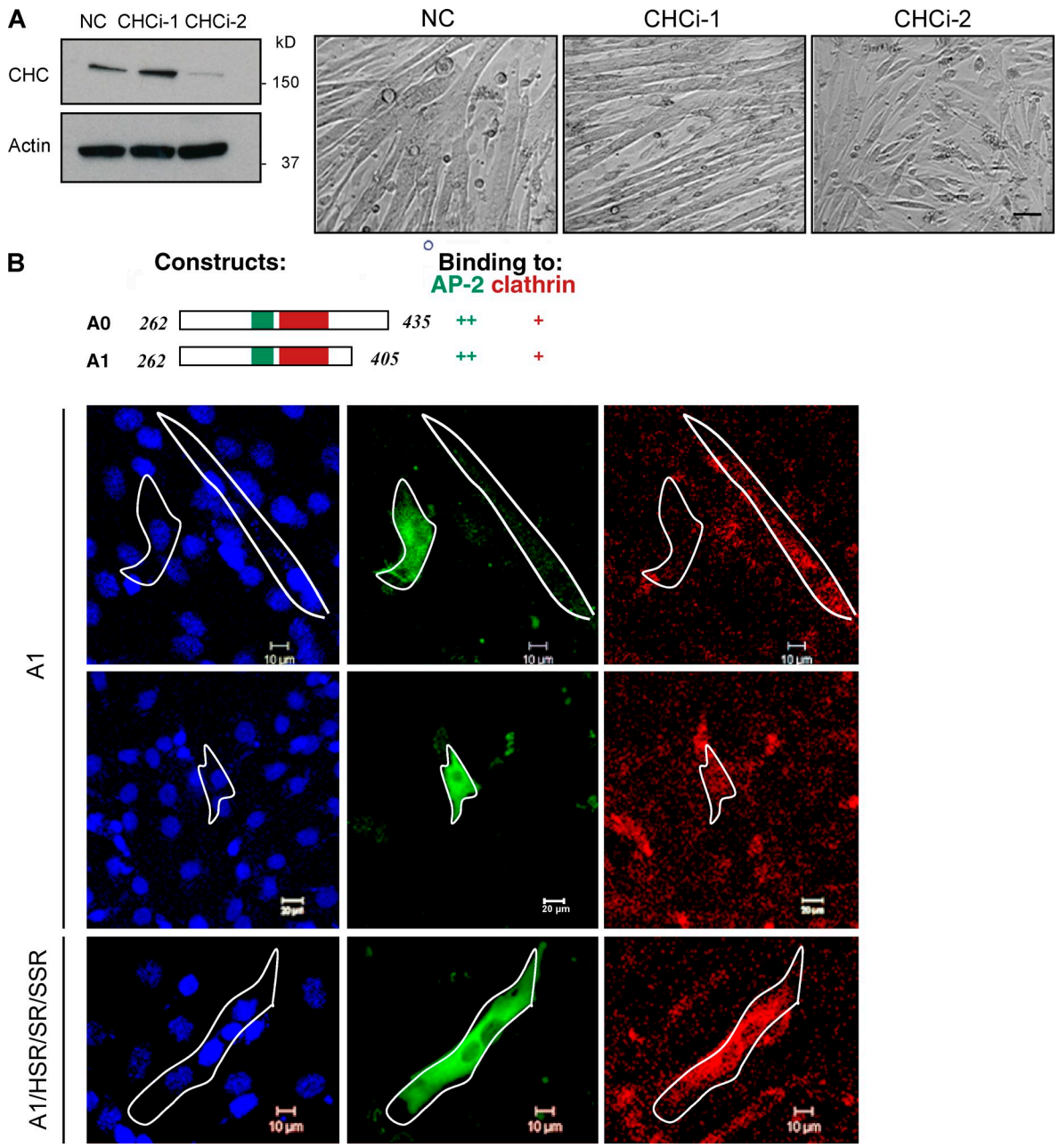

Figure 8. **Inhibition of endocytosis decreases myoblast fusion.** (A) siRNA knockdown of CHC was analyzed by Western blotting. Images of C2C12 cells transfected with negative control or two different CHC siRNAs were cultured for 96 h in differentiation media. Bar, 20 µm. (B) Effect of expression of an amphiphysin fragment that binds both clathrin and AP-2, and blocks endocytosis on the fusion of myoblast fusion. C2C12 cells were transfected with HA-tagged fragments of amphiphysin (green): wild-type A1 fragment and mutant fragment A1/HSR/SR/SSR that doesn't bind either clathrin or AP-2. 24 h after transfection, cells were differentiated for 3 d and then incubated with fluorescent transferrin (red) for 15 min before fixation and immunostaining for nuclei and HA-tag. Bars: (top and bottom) 10 µm; (middle) 20 µm.

demonstrate that endocytosis is indeed required, whether directly or indirectly, for the fusion of both cell types.

These observations suggest a fusion process involving both the formation of actin-rich structures at sites of cell–cell fusion, ensuring close contact between the membranes of fusing cells (Sens et al., 2010), and endocytosis, possibly contributing to the membrane fusion event itself. In fact, they point to a predominant role of impaired endocytosis in the defect of cell–cell fusion. We frequently observed coated pits opposite to the tip or on the sides of the actin-rich protrusions in the cell penetrated by such protrusions, raising the possibility that protrusions might, by analogy with the events leading to *Listeria* invasion (Bonazzi et al., 2011), be the result not only of pushing forces, but also of "pulling" forces produced by the invaded cell. Similar structures (cell protrusions facing clathrin-coated pits in the apposed cell) have been observed in this context (Bonazzi et al., 2011) and in developing tissues, where they are thought to represent underlying signaling by cell surface bound ligands and receptors (Bastiani and Goodman, 1984). Indeed, our EM observations are strikingly similar, in fact almost identical, to the

observations made by Bastiani and Goodman (1984) during neuronal development in the grasshopper embryo. These authors reported "filopodia" formation from a neuronal growth cone inserting deep into another growth cone and "inducing" coated pit formation (Bastiani and Goodman, 1984). This association of actin-rich protrusion and coated pits may therefore be a general mechanism involved in receptor–ligand-based cell–cell recognition, which would lead to cell–cell fusion only when the ligand and/or the receptor is a fusogen. The fact that we observe in OCPs that DC-STAMP is enriched in the membranes and colocalizes in part with CHC could indeed support this hypothesis. Nevertheless, the fact that we find endocytosis to be required suggests the presence of an additional membrane fusion event. Examples of clathrin-coated pits that engulf and then pinch off a protrusion of an adjacent cell (a process referred to as trans-endocytosis) have been previously described in non-fusing cells (Spacek and Harris, 2004), and the absence of dynamin also impairs this reaction (Hayashi et al., 2008). Here again the process would lead to cell–cell fusion only if, in addition to the receptor–ligand-based cell–cell recognition, a fusogen was present in the interacting membranes. It is therefore tempting to speculate that, in the presence of a receptor–ligand cell–cell interaction and of a fusogen in the membranes of one or both apposed cells, the constricting force of dynamin at the double membranes of the pit neck may help to induce fusion. Further studies will be required to test this hypothesis. Furthermore, our data from mixed cultures of DKO and CTL cells clearly shows that dynamin is required in both of the fusing cells, i.e., in the cell generating the actin-rich protrusion (invading) and in the cell forming the coated pits (invaded).

As demonstrated in the placenta for syncytins and in *C. elegans* for EFF1 (Mi et al., 2000; Frendo et al., 2003; Podbilewicz et al., 2006), the presence of specific fusogens in the plasma membrane of the fusing cells, possibly recognized by receptors at the surface of the apposed cell, plays an essential role in ensuring cell–cell recognition, cell–cell fusion, and close interaction of the two membranes. It is possible that this receptor–ligand interaction initiates a receptor-mediated clathrin- and dynamin-dependent endocytic event, ultimately causing fusion of the two membranes. Although internalization of DC-STAMP has been reported to contribute to OCP fusion (Mensah et al., 2010), it cannot be established whether endocytosis is triggering the membrane fusion event itself or is required for signaling events necessary for cell–cell fusion. Independent of which process is indeed occurring, our data firmly establishes that dynamin function and endocytic events are both required for the fusion of both OCPs and myoblasts.

Our findings significantly extend several recent observations. Members of the dynamin superfamily of GTPases, including atlastin, Mfn1, and Opa1, have been shown to participate in membrane remodeling events including organelle fusion (Hoppins et al., 2007; Hu et al., 2009; Orso et al., 2009; Westermann, 2011), which suggests a general involvement of dynamin-like proteins in membrane fusion or fission reactions. Studies of syncytium formation using viral fusogens and myoblasts have suggested that dynamin and its dynasore-sensitive GTPase activity (although dynasore is not specific for dynamin, see Park et al., 2013) are critical for fusion (Richard et al., 2011; Leikina et al., 2013). We extend these studies by showing that in primary OCPs, as in myoblasts, dynamin is required for cell fusion to occur. We also extend these findings by showing in vivo that osteoclast-targeted deletion of dynamin 1 and 2 leads to the formation of smaller and functionally impaired OCs. The importance of the actin cytoskeletal organization and of podosome-like structures in membrane fusion has also been previously suggested in myoblasts and OCPs (Chen et al., 2007; Kim et al., 2007; Laurin et al., 2008; Pajcini et al., 2008; Gonzalo et al., 2010; Sens et al., 2010; Oikawa et al., 2012) but a role for dynamin and/or endocytosis has never been identified. In addition, dynamin-interacting molecules—the small GTPase Rac1 and the invadopodia regulator Tks5/Fish—have been shown to be essential in myoblast and in osteoclast fusion, respectively (Charrasse et al., 2007; Vasyutina et al., 2009; Gonzalo et al., 2010; Haralalka et al., 2011; Oikawa et al., 2012), but again a link to dynamin function or endocytosis was not previously explored.

Finally, Sens et al. (2010) identified podosome-like invasive structures and suggested that these structures facilitated cell membrane juxtaposition and the formation of fusion pores during *Drosophila* myoblast fusion. More recently, Shilagardi et al. (2013) have reconstituted in vitro the *Drosophila* myoblast fusion process and demonstrated that actin-propelled invasive membrane protrusions drive fusogenic protein engagement during cell–cell fusion, and that both are required. Collectively, all these studies suggested a role for actin regulation in fusion, along with a role of fusogenic membrane proteins. However, with the exception of Leikina et al. (2013), the involvement of dynamin in the fusion process has not been investigated. We extend these findings by showing for the first time that endocytosis is required and that dynamin is required in both fusing cells during the OCP cell–cell fusion event.

Our findings could also help understand the fact that mutations in the PH domain of dynamin in humans leads to centronuclear myopathy (CNM; Bitoun et al., 2005), a muscle weakness disease in which myoblasts nuclei remain in the central region of the cytoplasm in the muscle fiber instead of migrating to the periphery of the cells. Our results raise the possibility that this myopathy could be related to the role of dynamin in myoblast fusion. We show here that introduction of one of the mutations (K562E, related to Charcot-Marie-Tooth [CMT] neuropathy disease) in the dynamin PH domain prevents the rescue of the defective fusion observed in *Dnm*-DKO;ERT OCPs, which suggests that the fusion process might be altered in the patients harboring this mutation and thereby be linked to the CNM and/or CMT phenotype. As *Dnm*-DKO mice are not viable, it has not been possible to explore whether muscle defects resembling CNM are observed in vivo in these animals. Further work will be necessary to address this question. Similarly, and since we found that in vivo osteoclast-targeted deletion of dynamin 1 and 2 reduces bone resorption and leads to an increase in bone density, whether patients harboring these mutations also exhibit some form of skeletal phenotype due to defective osteoclasts remains to be explored. Further studies will be required to address these important questions.

In conclusion, our results unequivocally demonstrate that dynamin function and endocytosis are required for the fusion of both OCPs and primary myoblasts.

Materials and methods

Antibodies

Antibodies used for immunoblot and immunofluorescence analysis were obtained from the following sources: mouse anti–dynamin 1/2 and mouse anti–dynamin 2 were from BD; rabbit anti–dynamin 2 was described previously (Ferguson et al., 2009); mouse anti–DC-STAMP, mouse anti-actin, mouse anti–cathepsin K, and rabbit anti–integrin β3 were from EMD Millipore; rabbit anti-Src and mouse anti-NFATc1 were from Santa Cruz Biotechnology, Inc.; mouse anti-vinculin was from Sigma-Aldrich; rabbit anti-CHC was from Abcam; anti–mouse and anti–rabbit IgG-HRP conjugates were from Promega; and Alexa Fluor 488– and 546–conjugated secondary antibodies were from Invitrogen.

Mice

The generation of CreER;*Dnm1*$^{flox/flox}$;*Dnm2*$^{flox/flox}$ mice has been described previously (Ferguson et al., 2009). In brief, *Dnm1*$^{flox/flox}$;*Dnm2*$^{flox/flox}$ mice (C57BL/6J-129S1/Sv) carrying conditional knockout alleles with exons 2–4 (Dnm1) and exon 2 (Dnm2) floxed were crossed with tamoxifen-inducible Cre mice (B6;129-Gt(ROSA)26Sortm1(cre/Esr1)Nat/J) (Badea et al., 2003). To generate Ctsk-Cre;*Dnm1*$^{flox/flox}$;*Dnm2*$^{flox/flox}$ mice, *Dnm1*$^{flox/flox}$;*Dnm2*$^{flox/flox}$ mice were crossed with Ctsk-Cre mice (Ctsktm1(cre)Ska/Ctsk+; C57BL/6), provided by S. Kato (University of Tokyo, Tokyo, Japan; Nakamura et al., 2007). Genotyping of recombinant mice was performed in-house by PCR analysis. All mice were housed at the Harvard Medical School and experimental protocols were approved by the Harvard Institutional Animal Care and Use Committee (IACUC).

Osteoclast culture and targeted deletion of endogenous dynamins

For in vitro osteoclast differentiation, primary bone marrow cells were isolated from tibiae and femora of ∼4–8-week-old mice and cultured under 5% CO_2 at 37 °C in α-MEM supplemented with 10% FBS, penicillin (100 U/ml), and streptomycin (100 µg/ml) in the presence of human M-CSF (30 ng/ml; R&D Systems) for 3 d on nontreated dishes. The resulting OCPs were lifted with 1 mM EDTA in PBS and replated and cultured on plastic dishes or on a glass coverslip with human RANKL (10 ng/ml; R&D Systems) and human M-CSF. Under these conditions, OCPs form multinucleated cells by day 2 and mature OCs with podosome belts by day 3. Targeted deletion of dynamins in OCs was accomplished by treating BMMs with 300 nM 4-OH tamoxifen (Sigma-Aldrich) in the presence of M-CSF for 1.5 d before differentiating with M-CSF and RANKL. The differentiated cells were either harvested for Western blotting or fixed with 4% formaldehyde/PBS and subjected to TRAP staining or immunofluorescence staining. To rescue DKO cells, BMMs derived from dynamin conditional KO mice were infected with lentivirus expressing the respective dynamin protein (pLenti-GFP-dynamin variants) or vector only. The endogenous dynamins were depleted by the addition of 300 nM of 4-OHT to the culture medium for 2 d before differentiation. Expression levels were determined by Western blot analysis. Inhibitors dynasore, monodansylcadaverine, and chlorpromazine (all from Sigma-Aldrich) were treated at day 2 of RANKL and M-CSF stimulation for 6 h before fixation due to their reversible inhibitory effects.

Myoblast culture

Primary mouse myoblasts were isolated from limbs of 4–5-d-old mice, cultured as described (Rando and Blau, 1994), and differentiated with low serum medium (5% horse serum in DMEM, supplemented with 100 U/ml penicillin and 100 µg/ml streptomycin) in 37 °C/5% CO_2, changing medium every other day. C2C12 mouse myoblasts were cultured in DMEM medium supplemented with 10% FBS, penicillin, and streptomycin, and differentiation was induced with 2% horse serum medium, referred to as DM.

Plasmids and lentiviral production and transduction

To express *Dnm2* WT or mutant constructs in BMMs, mouse N-terminal HA-tagged *Dnm2* constructs were cloned into pLenti-GFP (Addgene). To produce lentiviruses, 293T cells were transfected with lentiviral plasmids along with packaging plasmids using X-tremeGENE HP DNA Transfection Reagent (Roche) according to the manufacturer's protocol, and viral particles were collected after 48–72 h. BMMs were transduced with viral particles for 16 h in the presence of M-CSF and 8 µg/ml polybrene and, after 1 d of recovery, selected with antibiotics for transduced cells. Dnm2 shRNA lentiviral particles were purchased from Sigma-Aldrich, and CHC shRNA constructs were from OriGene.

RNAi

For siRNA transfection, BMMs or C2C12 myoblasts in proliferation were transfected with siRNA (50 nM/transfection) using Lipofectamine RNAiMAX (Invitrogen) according to the manufacturer's instructions. Cells were transfected again the next day and then 6 h after differentiation with RANKL and M-CSF. siRNAs were purchased from Integrated DNA Technologies (Dnm2) and Ambion (CHC). Lentiviral shRNAs with a puromycin resistance gene were produced or purchased from Sigma-Aldrich (Dnm2) and OriGene (CHC). BMMs or C2C12 myoblasts infected with lentiviruses were selected with puromycin and cultured 3–4 d for differentiation. Cells were then harvested for Western blot analyses or fixed for TRAP or H&E staining.

Quantitative RT-PCR analysis

Total RNA was extracted from osteoclast cultures by using an RNeasy Mini kit (QIAGEN) according to the manufacturer's protocol. RNA was quantified spectrophotometrically and then cDNA was synthesized from 1 µg of total RNA using the SuperScript VILO cDNA Synthesis kit (Invitrogen). Quantitative real-time PCR analysis was performed in a 96-well plate using an iCycler (Bio-Rad Laboratories). Glyceraldehyde 3-phosphate dehydrogenase (GAPDH) and 18 S ribosomal RNA (rRNA) were used for normalization.

Cell labeling for fusion assay

Adherent BMMs were removed from the dish by incubating with 1 mM EDTA in PBS, and the recovered cells were labeled with fluorescent dyes including lipophilic tracers DiI (red) or DiO (green) or membrane-permeant CellTracker Green CMFDA according to the manufacturer's protocol (Life Technologies). DiI- and DiO-labeled cells were mixed for fusion efficiency and DiI- and CellTracker Green–labeled cells were used to observe lipid mixing as well as fusion. Mixed cells were seeded on a glass coverslip, cultured with RANKL and m-CSF for 2 d, and fixed with 3.7% formaldehyde for confocal microscopy. To quantify the efficiency of fusion and lipid mixing using DiI and CellTracker Green, cell nuclei were labeled with DAPI. Cell images were taken from at least 10 randomly chosen fields and analyzed. As in the report of Leikina et al. (2013), the efficiency of multinucleation (syncytium formation) was quantified as the percentage of cell nuclei in multinucleated osteoclasts compared with the total number of cell nuclei and lipid mixing as a hemifusion marker as the percentage of nuclei in colabeled mononuclear or multinuclear cells compared with the number of singly labeled cells.

Bone resorption assay

BMMs were plated on dentin slices and cultured for 3 d with M-CSF and RANKL. Dentin slices were washed with water, incubated in 1 N NaOH for 1 min, and sonicated to remove cells. Resorption pits on dentin slices were visualized by 1% toluidine blue in 1% sodium borate, and pit surface areas were quantified using the OsteoMeasure program (OsteoMetrics). Results were normalized for osteoclast number, as measured by staining for TRAP activity and counting cells with more than three nuclei.

Western blot analysis

Cultured cells were washed with ice-cold PBS and lysed in modified radioimmunoprecipitation assay buffer (50 mM Tris-Cl, 150 mM NaCl, 1% Nonidet P-40, and 0.25% sodium deoxycholate) containing protease inhibitors (Complete; Roche). Cell lysates were incubated for 20 min at 4°C and the supernatant was clarified by centrifugation at 13,000 rpm for 15 min. 15–20 µg of samples were boiled in SDS-containing sample buffer under reducing conditions, and proteins were resolved by SDS-PAGE and transferred electrophoretically onto nitrocellulose membranes with a semidry system (Bio-Rad Laboratories). Membranes were blocked by incubation with 5% BSA in TBS with Tween 20 (TBST) and then incubated with primary antibodies. Membranes were then washed three times with TBST and incubated with HRP-conjugated secondary antibody diluted in TBST. Membranes were washed three times again with TBST and the protein bands were visualized with enhanced chemiluminescence reagents (GE Healthcare).

TRAP staining

In brief, differentiated osteoclasts were fixed with 4% paraformaldehyde in PBS and with 1:1 (vol/vol) ethanol/acetone before detection of TRAP activity.

Cells were incubated in 0.1 M sodium acetate buffer, pH 5, containing 50 mM sodium tartrate, 2 mM Naphtol AS-MX phosphate (Sigma-Aldrich), and 2 mM Fast Red Violet LB salt (Sigma-Aldrich) at RT until color developed and then rinsed in distilled water.

Immunofluorescence and confocal microscopy

Cells plated on FBS-coated coverslips or dentin slices were fixed with 3.7% formaldehyde in PBS for 10 min and washed in PBS. They were treated with ice-cold acetone and blocked with PBS containing 5% normal serum, 0.1% BSA, and 0.05% saponin. The cells were incubated with primary antibodies diluted in the above buffer for 1 h, washed, and incubated with secondary antibodies (Alexa Fluor 488, 568, or 647) for 1 h and washed again. F-actin was labeled with rhodamine phalloidin (Invitrogen) and nuclei were labeled with TO-PRO-3 (Invitrogen). Samples were mounted with FluorSave Reagent (EMD Millipore) or Prolong Gold antifade reagent with DAPI (Invitrogen). Images were obtained using a confocal microscope (LSM510; Carl Zeiss) equipped with a 40× oil-immersion objective lens (1.3 NA) or a 63× oil-immersion objective lens (1.4 NA), three visible wavelength lasers, and a META spectral emission detector. Images were taken at room temperature. Images were processed and analyzed with Photoshop (Adobe) and ImageJ (National Institutes of Health).

Live-cell imaging

To investigate actin podosome dynamics in cell–cell fusion, BMMs were plated on a Lab-Tek chambered coverglass (Thermo Fisher Scientific), transduced with LentiBrite GFP-β-actin lentivirus (EMD Millipore) according to the manufacturer's protocol, and stimulated with M-CSF and RANKL. Brightfield images and GFP images were collected in a 5% CO_2 humidified atmosphere at 37°C using a spinning disk confocal scanner (CSU-X1; Yokogawa) mounted on an inverted microscope (IX81; Olympus). Time-lapse images were taken at 2-min intervals over 16 h using a 60× 1.42 NA objective lens and an iXon3 897 EMCCD camera (Andor Technology). Acquired images were processed and analyzed with Photoshop (Adobe) and ImageJ. Cell tracking for migration was performed manually using the tracking function of the MTrackJ plugin of ImageJ.

Electron microscopy

Control and Dnm-DKO cultured on glass coverslips were fixed with 2.5% glutaraldehyde in 0.1 M sodium cacodylate buffer for 1 h at RT. The cells were postfixed in 1% OsO_4, 1.5% $K_4Fe(CN)_6$, and 0.1 M sodium cacodylate, en bloc stained with 0.5% uranyl magnesium acetate, dehydrated, embedded in Embed 812, and finally polymerized at 60°C for 24–48 h. Ultrathin sections were examined using a transmission electron microscope (CM10; Philips) at 80 kV, and images were obtained with a Morada megapixel CCD camera (Olympus).

Serum CTX

Quantitative determination of C-telopeptide fragments of Type I collagen in serum was performed using a Serum CrossLaps ELISA kit from Nordic Bioscience.

Histomorphometry

For histomorphometric analysis, mice were injected 7 and 2 d before sacrifice with calcein (20 mg/kg of body weight; Sigma-Aldrich) and demeclocycline (40 mg/kg of body weight; Sigma-Aldrich), respectively. The tibiae and femora of 6-wk-old *Dnm1*$^{fl/fl}$*;Dnm2*$^{fl/fl}$ and *Dnm1*$^{fl/fl}$*;Dnm2*$^{fl/fl}$;Ctsk-cre mice were collected and fixed in 3.7% PBS-buffered formaldehyde. For histomorphometric analysis, right tibiae were embedded in methyl methacrylate, and toluidine blue and von Kossa stainings were performed on 5-µm sagittal sections. For TRAP staining, tibiae were embedded in paraffin after decalcification. All histological images were obtained using a microscope (Eclipse E800; Nikon) with a 20× (NA 0.50) objective lens fitted with a camera (DP71) and software (DP controller; Olympus). Quantitative bone histomorphometric measurements were performed according to standardized protocols (Parfitt et al., 1987) using the OsteoMeasure system (OsteoMetrics).

µCT imaging and analysis

Scanco Medical µCT35 with an isotropic voxel size of 7 µm was used to image the distal femur. Scans were conducted with an x-ray tube potential of 70 kVP, an x-ray intensity of 0.145 mA, and an integration time of 600 ms per tomographic projection. From the scans, a region starting 280 µm proximal to the distal femoral growth plate and extending trabecular bone 2.1 mm was selected for trabecular bone analysis. A Gaussian filter using a fixed threshold at 26% of maximal grayscale value was applied to the femur images. Three-dimensional images were reconstructed from the two-dimensional images from the contoured regions.

Statistical analyses

Quantitative data are shown as the means ± SD or SEM, and p-values <0.05 were considered statistically significant. Statistical analyses were performed using a Student's *t* test or analysis of variance (ANOVA) followed by a *t* test, and p-values of <0.05 were considered significant. Results are representative examples of more than three independent experiments.

Online supplemental material

Fig. S1 shows the effect of dynamin depletion on cell motility, dynamin knockout efficiency in osteoclasts derived from Ctsk-cre; Dnm1$^{fl/fl}$Dnm2$^{fl/fl}$ mice, and impaired osteoclast multinucleation by dynamin inhibitor dynasore. Fig. S2 shows the formation of podosome clusters during cell–cell fusion. Fig. S3 shows that intracellular localization of CHC, endophilin, and DC-STAMP is decreased in Dnm-DKO osteoclasts; and that endocytosis inhibitors impair osteoclast fusion. Fig. S4 shows the expression level of dynamin isoforms during myoblast differentiation, the effect of dynamin 2 knockdown on myoblast fusion, the presence of protrusive structures at myoblast cell–cell fusion sites, and the effect of endocytosis inhibitors on myoblast fusion. Table S1 shows histomorphometric analysis data from 6-wk-old Ctsk-cre;Dnm1$^{fl/fl}$Dnm2$^{fl/fl}$ mice and control littermates. Online supplemental material is available at http://www.jcb.org/cgi/content/full/jcb.201401137/DC1.

We thank Dr. William C. Horne for editing, Dr. Francesca Gori and Flavia Pinho for help with lentiviral dynamin constructs, and Dr. Shigeaki Kato for providing Cathepsin K cre mice. Confocal analysis and µCT analysis were performed at the Harvard NeuroDiscovery Center and at the MicroCT facility at Harvard School of Dental Medicine, respectively.

This work was supported by the National Institutes of Health grants to R. Baron (National Institute of Arthritis and Musculoskeletal and Skin Diseases, RO1AR 054450, and AR062054) and to P. De Camilli (R37NS036251).

The authors declare no competing financial interests.

Submitted: 30 January 2014
Accepted: 2 September 2014

References

Abmayr, S.M., and G.K. Pavlath. 2012. Myoblast fusion: lessons from flies and mice. *Development*. 139:641–656. http://dx.doi.org/10.1242/dev.068353

Badea, T.C., Y. Wang, and J. Nathans. 2003. A noninvasive genetic/pharmacologic strategy for visualizing cell morphology and clonal relationships in the mouse. *J. Neurosci.* 23:2314–2322.

Baldassarre, M., A. Pompeo, G. Beznoussenko, C. Castaldi, S. Cortellino, M.A. McNiven, A. Luini, and R. Buccione. 2003. Dynamin participates in focal extracellular matrix degradation by invasive cells. *Mol. Biol. Cell*. 14:1074–1084. http://dx.doi.org/10.1091/mbc.E02-05-0308

Bastiani, M.J., and C.S. Goodman. 1984. Neuronal growth cones: specific interactions mediated by filopodial insertion and induction of coated vesicles. *Proc. Natl. Acad. Sci. USA*. 81:1849–1853. http://dx.doi.org/10.1073/pnas.81.6.1849

Berger, S., G. Schäfer, D.A. Kesper, A. Holz, T. Eriksson, R.H. Palmer, L. Beck, C. Klämbt, R. Renkawitz-Pohl, and S.F. Onel. 2008. WASP and SCAR have distinct roles in activating the Arp2/3 complex during myoblast fusion. *J. Cell Sci.* 121:1303–1313. http://dx.doi.org/10.1242/jcs.022269

Bitoun, M., S. Maugenre, P.Y. Jeannet, E. Lacène, X. Ferrer, P. Laforêt, J.J. Martin, J. Laporte, H. Lochmüller, A.H. Beggs, et al. 2005. Mutations in dynamin 2 cause dominant centronuclear myopathy. *Nat. Genet.* 37:1207–1209. http://dx.doi.org/10.1038/ng1657

Bonazzi, M., L. Vasudevan, A. Mallet, M. Sachse, A. Sartori, M.C. Prevost, A. Roberts, S.B. Taner, J.D. Wilbur, F.M. Brodsky, and P. Cossart. 2011. Clathrin phosphorylation is required for actin recruitment at sites of bacterial adhesion and internalization. *J. Cell Biol.* 195:525–536. http://dx.doi.org/10.1083/jcb.201105152

Bruzzaniti, A., L. Neff, A. Sanjay, W.C. Horne, P. De Camilli, and R. Baron. 2005. Dynamin forms a Src kinase-sensitive complex with Cbl and regulates podosomes and osteoclast activity. *Mol. Biol. Cell*. 16:3301–3313. http://dx.doi.org/10.1091/mbc.E04-12-1117

Bruzzaniti, A., L. Neff, A. Sandoval, L. Du, W.C. Horne, and R. Baron. 2009. Dynamin reduces Pyk2 Y402 phosphorylation and SRC binding in osteoclasts. *Mol. Cell. Biol.* 29:3644–3656. http://dx.doi.org/10.1128/MCB.00851-08

Cao, H., J.D. Orth, J. Chen, S.G. Weller, J.E. Heuser, and M.A. McNiven. 2003. Cortactin is a component of clathrin-coated pits and participates in receptor-mediated endocytosis. *Mol. Cell. Biol.* 23:2162–2170. http://dx.doi.org/10.1128/MCB.23.6.2162-2170.2003

Chappie, J.S., J.A. Mears, S. Fang, M. Leonard, S.L. Schmid, R.A. Milligan, J.E. Hinshaw, and F. Dyda. 2011. A pseudoatomic model of the dynamin polymer identifies a hydrolysis-dependent powerstroke. *Cell*. 147:209–222. http://dx.doi.org/10.1016/j.cell.2011.09.003

Charrasse, S., F. Comunale, M. Fortier, E. Portales-Casamar, A. Debant, and C. Gauthier-Rouvière. 2007. M-cadherin activates Rac1 GTPase through the Rho-GEF trio during myoblast fusion. *Mol. Biol. Cell*. 18:1734–1743. http://dx.doi.org/10.1091/mbc.E06-08-0766

Chen, E.H., E. Grote, W. Mohler, and A. Vignery. 2007. Cell-cell fusion. *FEBS Lett.* 581:2181–2193. http://dx.doi.org/10.1016/j.febslet.2007.03.033

Chernomordik, L.V., E. Leikina, M.M. Kozlov, V.A. Frolov, and J. Zimmerberg. 1999. Structural intermediates in influenza haemagglutinin-mediated fusion. *Mol. Membr. Biol.* 16:33–42. http://dx.doi.org/10.1080/096876899294733

Damke, H., T. Baba, D.E. Warnock, and S.L. Schmid. 1994. Induction of mutant dynamin specifically blocks endocytic coated vesicle formation. *J. Cell Biol.* 127:915–934. http://dx.doi.org/10.1083/jcb.127.4.915

Destaing, O., S.M. Ferguson, A. Grichine, C. Oddou, P. De Camilli, C. Albiges-Rizo, and R. Baron. 2013. Essential function of dynamin in the invasive properties and actin architecture of v-Src induced podosomes/invadosomes. *PLoS ONE*. 8:e77956. http://dx.doi.org/10.1371/journal.pone.0077956

Dupressoir, A., C. Lavialle, and T. Heidmann. 2012. From ancestral infectious retroviruses to bona fide cellular genes: role of the captured syncytins in placentation. *Placenta*. 33:663–671. http://dx.doi.org/10.1016/j.placenta.2012.05.005

Faelber, K., Y. Posor, S. Gao, M. Held, Y. Roske, D. Schulze, V. Haucke, F. Noé, and O. Daumke. 2011. Crystal structure of nucleotide-free dynamin. *Nature*. 477:556–560. http://dx.doi.org/10.1038/nature10369

Ferguson, S.M., and P. De Camilli. 2012. Dynamin, a membrane-remodelling GTPase. *Nat. Rev. Mol. Cell Biol.* 13:75–88.

Ferguson, K.M., M.A. Lemmon, J. Schlessinger, and P.B. Sigler. 1994. Crystal structure at 2.2 A resolution of the pleckstrin homology domain from human dynamin. *Cell*. 79:199–209. http://dx.doi.org/10.1016/0092-8674(94)90190-2

Ferguson, S.M., A. Raimondi, S. Paradise, H. Shen, K. Mesaki, A. Ferguson, O. Destaing, G. Ko, J. Takasaki, O. Cremona, et al. 2009. Coordinated actions of actin and BAR proteins upstream of dynamin at endocytic clathrin-coated pits. *Dev. Cell*. 17:811–822. (published erratum appears in *Dev. Cell*. 2010. 18:332) http://dx.doi.org/10.1016/j.devcel.2009.11.005

Ford, M.G., S. Jenni, and J. Nunnari. 2011. The crystal structure of dynamin. *Nature*. 477:561–566. http://dx.doi.org/10.1038/nature10441

Frendo, J.L., D. Olivier, V. Cheynet, J.L. Blond, O. Bouton, M. Vidaud, M. Rabreau, D. Evain-Brion, and F. Mallet. 2003. Direct involvement of HERV-W Env glycoprotein in human trophoblast cell fusion and differentiation. *Mol. Cell. Biol.* 23:3566–3574. http://dx.doi.org/10.1128/MCB.23.10.3566-3574.2003

Gonzalo, P., M.C. Guadamillas, M.V. Hernández-Riquer, A. Pollán, A. Grande-García, R.A. Bartolomé, A. Vasanji, C. Ambrogio, R. Chiarle, J. Teixidó, et al. 2010. MT1-MMP is required for myeloid cell fusion via regulation of Rac1 signaling. *Dev. Cell*. 18:77–89. http://dx.doi.org/10.1016/j.devcel.2009.11.012

Grassart, A., A.T. Cheng, S.H. Hong, F. Zhang, N. Zenzer, Y. Feng, D.M. Briner, G.D. Davis, D. Malkov, and D.G. Drubin. 2014. Actin and dynamin2 dynamics and interplay during clathrin-mediated endocytosis. *J. Cell Biol.* 205:721–735. http://dx.doi.org/10.1083/jcb.201403041

Gruenbaum-Cohen, Y., I. Harel, K.B. Umansky, E. Tzahor, S.B. Snapper, B.Z. Shilo, and E.D. Schejter. 2012. The actin regulator N-WASp is required for muscle-cell fusion in mice. *Proc. Natl. Acad. Sci. USA*. 109:11211–11216. http://dx.doi.org/10.1073/pnas.1116065109

Haralalka, S., C. Shelton, H.N. Cartwright, E. Katzfey, E. Janzen, and S.M. Abmayr. 2011. Asymmetric Mbc, active Rac1 and F-actin foci in the fusion-competent myoblasts during myoblast fusion in *Drosophila*. *Development*. 138:1551–1562. http://dx.doi.org/10.1242/dev.057653

Hayashi, M., A. Raimondi, E. O'Toole, S. Paradise, C. Collesi, O. Cremona, S.M. Ferguson, and P. De Camilli. 2008. Cell- and stimulus-dependent heterogeneity of synaptic vesicle endocytic recycling mechanisms revealed by studies of dynamin 1-null neurons. *Proc. Natl. Acad. Sci. USA*. 105:2175–2180. http://dx.doi.org/10.1073/pnas.0712171105

Helming, L., and S. Gordon. 2009. Molecular mediators of macrophage fusion. *Trends Cell Biol.* 19:514–522. http://dx.doi.org/10.1016/j.tcb.2009.07.005

Hinshaw, J.E., and S.L. Schmid. 1995. Dynamin self-assembles into rings suggesting a mechanism for coated vesicle budding. *Nature*. 374:190–192. http://dx.doi.org/10.1038/374190a0

Hoppins, S., L. Lackner, and J. Nunnari. 2007. The machines that divide and fuse mitochondria. *Annu. Rev. Biochem.* 76:751–780. http://dx.doi.org/10.1146/annurev.biochem.76.071905.090048

Hu, J., Y. Shibata, P.P. Zhu, C. Voss, N. Rismanchi, W.A. Prinz, T.A. Rapoport, and C. Blackstone. 2009. A class of dynamin-like GTPases involved in the generation of the tubular ER network. *Cell*. 138:549–561. http://dx.doi.org/10.1016/j.cell.2009.05.025

Itoh, T., K.S. Erdmann, A. Roux, B. Habermann, H. Werner, and P. De Camilli. 2005. Dynamin and the actin cytoskeleton cooperatively regulate plasma membrane invagination by BAR and F-BAR proteins. *Dev. Cell*. 9:791–804. http://dx.doi.org/10.1016/j.devcel.2005.11.005

Jurdic, P., F. Saltel, A. Chabadel, and O. Destaing. 2006. Podosome and sealing zone: specificity of the osteoclast model. *Eur. J. Cell Biol.* 85:195–202. http://dx.doi.org/10.1016/j.ejcb.2005.09.008

Kawada, K., G. Upadhyay, S. Ferandon, S. Janarthanan, M. Hall, J.P. Vilardaga, and V. Yajnik. 2009. Cell migration is regulated by platelet-derived growth factor receptor endocytosis. *Mol. Cell. Biol.* 29:4508–4518. http://dx.doi.org/10.1128/MCB.00015-09

Kessels, M.M., A.E. Engqvist-Goldstein, D.G. Drubin, and B. Qualmann. 2001. Mammalian Abp1, a signal-responsive F-actin-binding protein, links the actin cytoskeleton to endocytosis via the GTPase dynamin. *J. Cell Biol.* 153:351–366. http://dx.doi.org/10.1083/jcb.153.2.351

Kesper, D.A., C. Stute, D. Buttgereit, N. Kreisköther, S. Vishnu, K.F. Fischbach, and R. Renkawitz-Pohl. 2007. Myoblast fusion in Drosophila melanogaster is mediated through a fusion-restricted myogenic-adhesive structure (FuRMAS). *Dev. Dyn.* 236:404–415. http://dx.doi.org/10.1002/dvdy.21035

Kim, S., K. Shilagardi, S. Zhang, S.N. Hong, K.L. Sens, J. Bo, G.A. Gonzalez, and E.H. Chen. 2007. A critical function for the actin cytoskeleton in targeted exocytosis of prefusion vesicles during myoblast fusion. *Dev. Cell*. 12:571–586. http://dx.doi.org/10.1016/j.devcel.2007.02.019

Kim, K., S.H. Lee, J. Ha Kim, Y. Choi, and N. Kim. 2008. NFATc1 induces osteoclast fusion via up-regulation of Atp6v0d2 and the dendritic cell-specific transmembrane protein (DC-STAMP). *Mol. Endocrinol.* 22:176–185. http://dx.doi.org/10.1210/me.2007-0237

Krueger, E.W., J.D. Orth, H. Cao, and M.A. McNiven. 2003. A dynamin-cortactin-Arp2/3 complex mediates actin reorganization in growth factor-stimulated cells. *Mol. Biol. Cell*. 14:1085–1096. http://dx.doi.org/10.1091/mbc.E02-08-0466

Laurin, M., N. Fradet, A. Blangy, A. Hall, K. Vuori, and J.F. Côté. 2008. The atypical Rac activator Dock180 (Dock1) regulates myoblast fusion in vivo. *Proc. Natl. Acad. Sci. USA*. 105:15446–15451. http://dx.doi.org/10.1073/pnas.0805546105

Lee, A., D.W. Frank, M.S. Marks, and M.A. Lemmon. 1999. Dominant-negative inhibition of receptor-mediated endocytosis by a dynamin-1 mutant with a defective pleckstrin homology domain. *Curr. Biol.* 9:261–265. http://dx.doi.org/10.1016/S0960-9822(99)80115-8

Lee, S.H., J. Rho, D. Jeong, J.Y. Sul, T. Kim, N. Kim, J.S. Kang, T. Miyamoto, T. Suda, S.K. Lee, et al. 2006. v-ATPase V0 subunit d2-deficient mice exhibit impaired osteoclast fusion and increased bone formation. *Nat. Med.* 12:1403–1409. http://dx.doi.org/10.1038/nm1514

Leikina, E., K. Melikov, S. Sanyal, S.K. Verma, B. Eun, C. Gebert, K. Pfeifer, V.A. Lizunov, M.M. Kozlov, and L.V. Chernomordik. 2013. Extracellular annexins and dynamin are important for sequential steps in myoblast fusion. *J. Cell Biol.* 200:109–123. http://dx.doi.org/10.1083/jcb.201207012

Linder, S., and M. Aepfelbacher. 2003. Podosomes: adhesion hot-spots of invasive cells. *Trends Cell Biol.* 13:376–385. http://dx.doi.org/10.1016/S0962-8924(03)00128-4

Liu, Y.W., M.C. Surka, T. Schroeter, V. Lukiyanchuk, and S.L. Schmid. 2008. Isoform and splice-variant specific functions of dynamin-2 revealed by analysis of conditional knock-out cells. *Mol. Biol. Cell*. 19:5347–5359. http://dx.doi.org/10.1091/mbc.E08-08-0890

Mbalaviele, G., P. Orcel, C. Morieux, P.J. Nijweide, and M.C. de Vernejoul. 1995. Osteoclast formation from human cord blood mononuclear cells co-cultured with mice embryonic metatarsals in the presence of M-CSF. *Bone*. 16:171–177. http://dx.doi.org/10.1016/8756-3282(95)80029-P

McNiven, M.A., L. Kim, E.W. Krueger, J.D. Orth, H. Cao, and T.W. Wong. 2000. Regulated interactions between dynamin and the actin-binding

protein cortactin modulate cell shape. *J. Cell Biol.* 151:187–198. http://dx.doi.org/10.1083/jcb.151.1.187

Mensah, K.A., C.T. Ritchlin, and E.M. Schwarz. 2010. RANKL induces heterogeneous DC-STAMP(lo) and DC-STAMP(hi) osteoclast precursors of which the DC-STAMP(lo) precursors are the master fusogens. *J. Cell. Physiol.* 223:76–83.

Mi, S., X. Lee, X. Li, G.M. Veldman, H. Finnerty, L. Racie, E. LaVallie, X.Y. Tang, P. Edouard, S. Howes, et al. 2000. Syncytin is a captive retroviral envelope protein involved in human placental morphogenesis. *Nature*. 403:785–789. http://dx.doi.org/10.1038/35001608

Mohler, W.A., G. Shemer, J.J. del Campo, C. Valansi, E. Opoku-Serebuoh, V. Scranton, N. Assaf, J.G. White, and B. Podbilewicz. 2002. The type I membrane protein EFF-1 is essential for developmental cell fusion. *Dev. Cell*. 2:355–362. http://dx.doi.org/10.1016/S1534-5807(02)00129-6

Mooren, O.L., T.I. Kotova, A.J. Moore, and D.A. Schafer. 2009. Dynamin2 GTPase and cortactin remodel actin filaments. *J. Biol. Chem.* 284:23995–24005. http://dx.doi.org/10.1074/jbc.M109.024398

Murphy, D.A., and S.A. Courtneidge. 2011. The 'ins' and 'outs' of podosomes and invadopodia: characteristics, formation and function. *Nat. Rev. Mol. Cell Biol.* 12:413–426. http://dx.doi.org/10.1038/nrm3141

Nakamura, T., Y. Imai, T. Matsumoto, S. Sato, K. Takeuchi, K. Igarashi, Y. Harada, Y. Azuma, A. Krust, Y. Yamamoto, et al. 2007. Estrogen prevents bone loss via estrogen receptor alpha and induction of Fas ligand in osteoclasts. *Cell*. 130:811–823. http://dx.doi.org/10.1016/j.cell.2007.07.025

Ochoa, G.C., V.I. Slepnev, L. Neff, N. Ringstad, K. Takei, L. Daniell, W. Kim, H. Cao, M. McNiven, R. Baron, and P. De Camilli. 2000. A functional link between dynamin and the actin cytoskeleton at podosomes. *J. Cell Biol.* 150:377–389. http://dx.doi.org/10.1083/jcb.150.2.377

Oikawa, T., M. Oyama, H. Kozuka-Hata, S. Uehara, N. Udagawa, H. Saya, and K. Matsuo. 2012. Tks5-dependent formation of circumferential podosomes/invadopodia mediates cell-cell fusion. *J. Cell Biol.* 197:553–568. http://dx.doi.org/10.1083/jcb.201111116

Oren-Suissa, M., and B. Podbilewicz. 2007. Cell fusion during development. *Trends Cell Biol.* 17:537–546. http://dx.doi.org/10.1016/j.tcb.2007.09.004

Orso, G., D. Pendin, S. Liu, J. Tosetto, T.J. Moss, J.E. Faust, M. Micaroni, A. Egorova, A. Martinuzzi, J.A. McNew, and A. Daga. 2009. Homotypic fusion of ER membranes requires the dynamin-like GTPase atlastin. *Nature*. 460:978–983. http://dx.doi.org/10.1038/nature08280

Oursler, M.J. 2010. Recent advances in understanding the mechanisms of osteoclast precursor fusion. *J. Cell. Biochem.* 110:1058–1062. http://dx.doi.org/10.1002/jcb.22640

Pajcini, K.V., J.H. Pomerantz, O. Alkan, R. Doyonnas, and H.M. Blau. 2008. Myoblasts and macrophages share molecular components that contribute to cell-cell fusion. *J. Cell Biol.* 180:1005–1019. http://dx.doi.org/10.1083/jcb.200707191

Park, R.J., H. Shen, L. Liu, X. Liu, S.M. Ferguson, and P. De Camilli. 2013. Dynamin triple knockout cells reveal off target effects of commonly used dynamin inhibitors. *J. Cell Sci.* 126:5305–5312. http://dx.doi.org/10.1242/jcs.138578

Parfitt, A.M., M.K. Drezner, F.H. Glorieux, J.A. Kanis, H. Malluche, P.J. Meunier, S.M. Ott, and R.R. Recker. 1987. Bone histomorphometry: standardization of nomenclature, symbols, and units. Report of the ASBMR Histomorphometry Nomenclature Committee. *J. Bone Miner. Res.* 2:595–610. http://dx.doi.org/10.1002/jbmr.5650020617

Pérez-Vargas, J., T. Krey, C. Valansi, O. Avinoam, A. Haouz, M. Jamin, H. Raveh-Barak, B. Podbilewicz, and F.A. Rey. 2014. Structural basis of eukaryotic cell-cell fusion. *Cell*. 157:407–419. http://dx.doi.org/10.1016/j.cell.2014.02.020

Pirraglia, C., R. Jattani, and M.M. Myat. 2006. Rac function in epithelial tube morphogenesis. *Dev. Biol.* 290:435–446. http://dx.doi.org/10.1016/j.ydbio.2005.12.005

Podbilewicz, B., E. Leikina, A. Sapir, C. Valansi, M. Suissa, G. Shemer, and L.V. Chernomordik. 2006. The *C. elegans* developmental fusogen EFF-1 mediates homotypic fusion in heterologous cells and in vivo. *Dev. Cell*. 11:471–481. http://dx.doi.org/10.1016/j.devcel.2006.09.004

Rando, T.A., and H.M. Blau. 1994. Primary mouse myoblast purification, characterization, and transplantation for cell-mediated gene therapy. *J. Cell Biol.* 125:1275–1287. http://dx.doi.org/10.1083/jcb.125.6.1275

Richard, J.P., E. Leikina, R. Langen, W.M. Henne, M. Popova, T. Balla, H.T. McMahon, M.M. Kozlov, and L.V. Chernomordik. 2011. Intracellular curvature-generating proteins in cell-to-cell fusion. *Biochem. J.* 440:185–193. http://dx.doi.org/10.1042/BJ20111243

Saginario, C., H. Sterling, C. Beckers, R. Kobayashi, M. Solimena, E. Ullu, and A. Vignery. 1998. MFR, a putative receptor mediating the fusion of macrophages. *Mol. Cell. Biol.* 18:6213–6223.

Sapir, A., J. Choi, E. Leikina, O. Avinoam, C. Valansi, L.V. Chernomordik, A.P. Newman, and B. Podbilewicz. 2007. AFF-1, a FOS-1-regulated fusogen, mediates fusion of the anchor cell in *C. elegans*. *Dev. Cell*. 12:683–698. http://dx.doi.org/10.1016/j.devcel.2007.03.003

Schafer, D.A., S.A. Weed, D. Binns, A.V. Karginov, J.T. Parsons, and J.A. Cooper. 2002. Dynamin2 and cortactin regulate actin assembly and filament organization. *Curr. Biol.* 12:1852–1857. http://dx.doi.org/10.1016/S0960-9822(02)01228-9

Schlunck, G., H. Damke, W.B. Kiosses, N. Rusk, M.H. Symons, C.M. Waterman-Storer, S.L. Schmid, and M.A. Schwartz. 2004. Modulation of Rac localization and function by dynamin. *Mol. Biol. Cell*. 15:256–267. http://dx.doi.org/10.1091/mbc.E03-01-0019

Sens, K.L., S. Zhang, P. Jin, R. Duan, G. Zhang, F. Luo, L. Parachini, and E.H. Chen. 2010. An invasive podosome-like structure promotes fusion pore formation during myoblast fusion. *J. Cell Biol.* 191:1013–1027. http://dx.doi.org/10.1083/jcb.201006006

Shilagardi, K., S. Li, F. Luo, F. Marikar, R. Duan, P. Jin, J.H. Kim, K. Murnen, and E.H. Chen. 2013. Actin-propelled invasive membrane protrusions promote fusogenic protein engagement during cell-cell fusion. *Science*. 340:359–363. http://dx.doi.org/10.1126/science.1234781

Slepnev, V.I., G.C. Ochoa, M.H. Butler, D. Grabs, and P. De Camilli. 1998. Role of phosphorylation in regulation of the assembly of endocytic coat complexes. *Science*. 281:821–824. http://dx.doi.org/10.1126/science.281.5378.821

Slepnev, V.I., G.C. Ochoa, M.H. Butler, and P. De Camilli. 2000. Tandem arrangement of the clathrin and AP-2 binding domains in amphiphysin 1 and disruption of clathrin coat function by amphiphysin fragments comprising these sites. *J. Biol. Chem.* 275:17583–17589. http://dx.doi.org/10.1074/jbc.M910430199

Spacek, J., and K.M. Harris. 2004. Trans-endocytosis via spinules in adult rat hippocampus. *J. Neurosci.* 24:4233–4241. http://dx.doi.org/10.1523/JNEUROSCI.0287-04.2004

Takayanagi, H., S. Kim, T. Koga, H. Nishina, M. Isshiki, H. Yoshida, A. Saiura, M. Isobe, T. Yokochi, J. Inoue, et al. 2002. Induction and activation of the transcription factor NFATc1 (NFAT2) integrate RANKL signaling in terminal differentiation of osteoclasts. *Dev. Cell*. 3:889–901. http://dx.doi.org/10.1016/S1534-5807(02)00369-6

Takei, K., P.S. McPherson, S.L. Schmid, and P. De Camilli. 1995. Tubular membrane invaginations coated by dynamin rings are induced by GTP-γ S in nerve terminals. *Nature*. 374:186–190. http://dx.doi.org/10.1038/374186a0

Taylor, M.J., M. Lampe, and C.J. Merrifield. 2012. A feedback loop between dynamin and actin recruitment during clathrin-mediated endocytosis. *PLoS Biol.* 10:e1001302. http://dx.doi.org/10.1371/journal.pbio.1001302

Vallis, Y., P. Wigge, B. Marks, P.R. Evans, and H.T. McMahon. 1999. Importance of the pleckstrin homology domain of dynamin in clathrin-mediated endocytosis. *Curr. Biol.* 9:257–263. http://dx.doi.org/10.1016/S0960-9822(99)80114-6

Vasyutina, E., B. Martarelli, C. Brakebusch, H. Wende, and C. Birchmeier. 2009. The small G-proteins Rac1 and Cdc42 are essential for myoblast fusion in the mouse. *Proc. Natl. Acad. Sci. USA*. 106:8935–8940. http://dx.doi.org/10.1073/pnas.0902501106

Vignery, A. 2005. Macrophage fusion: the making of osteoclasts and giant cells. *J. Exp. Med.* 202:337–340. http://dx.doi.org/10.1084/jem.20051123

Westermann, B. 2011. Organelle dynamics: ER embraces mitochondria for fission. *Curr. Biol*. 21:R922–R924. http://dx.doi.org/10.1016/j.cub.2011.10.010

Witke, W., A.V. Podtelejnikov, A. Di Nardo, J.D. Sutherland, C.B. Gurniak, C. Dotti, and M. Mann. 1998. In mouse brain profilin I and profilin II associate with regulators of the endocytic pathway and actin assembly. *EMBO J.* 17:967–976. http://dx.doi.org/10.1093/emboj/17.4.967

Yagi, M., T. Miyamoto, Y. Sawatani, K. Iwamoto, N. Hosogane, N. Fujita, K. Morita, K. Ninomiya, T. Suzuki, K. Miyamoto, et al. 2005. DC-STAMP is essential for cell-cell fusion in osteoclasts and foreign body giant cells. *J. Exp. Med.* 202:345–351. http://dx.doi.org/10.1084/jem.20050645

Yang, M., M.J. Birnbaum, C.A. MacKay, A. Mason-Savas, B. Thompson, and P.R. Odgren. 2008. Osteoclast stimulatory transmembrane protein (OC-STAMP), a novel protein induced by RANKL that promotes osteoclast differentiation. *J. Cell. Physiol.* 215:497–505. http://dx.doi.org/10.1002/jcp.21331

Zheng, J., S.M. Cahill, M.A. Lemmon, D. Fushman, J. Schlessinger, and D. Cowburn. 1996. Identification of the binding site for acidic phospholipids on the pH domain of dynamin: implications for stimulation of GTPase activity. *J. Mol. Biol.* 255:14–21. http://dx.doi.org/10.1006/jmbi.1996.0002

Zhao, Q., X. Wang, Y. Liu, A. He, and R. Jia. 2010. NFATc1: functions in osteoclasts. *Int. J. Biochem. Cell Biol.* 42:576–579. http://dx.doi.org/10.1016/j.biocel.2009.12.018